

# Supplementary Information for

## ‘Serological imprinting and vaccination history shape adult influenza antibody landscapes and H5N1 cross-reactivity’

This Supplementary Information accompanies the manuscript ‘Serological imprinting and vaccination history shape adult influenza antibody landscapes and H5N1 cross-reactivity’ by Wilson K.K. et al.

Submitted to *Nature Communications* (2026)

### *Table of Contents*

<b>Overview of Supplementary Information .....</b>	<b>3</b>
<b>Supplemental Tables .....</b>	<b>3</b>
Table S1. Influenza Vaccination cohort – Clinical and demographic information..	3
Table S2. Influenza Infection cohort – Clinical and demographic information. ....	3
Table S3. Antigen and bead information.....	3
Table S4. Egg-adapted mutations in hemagglutinin antigens.....	4
Table S5. Linear and logistic regression data on binding responses by year of birth. .....	4
<b>Supplemental Figures .....</b>	<b>5</b>
Figure S1. Influenza-like illnesses (ILI), subtypes, and vaccine composition. ....	7
Figure S2. Phylogenetic relatedness of used hemagglutinin antigens. ....	9
Figure S3. Comparability of signals obtained in multiplex versus singleplex. ....	11
Figure S4. Two-Serum Dilution Strategy for high-throughput immunoprofiling with high resolution.....	13
Figure S5. Development and optimization of an Ig isotype and subclass-specific binding assay.....	15
Figure S6. Antibody subclass-specific binding profiles in infection cohort participant #1. ....	17
Figure S7. Antibody subclass-specific binding profiles in infection cohort participant #2. ....	19

Figure S8. Antibody subclass-specific binding profiles in infection cohort participant #3. ....	21
Figure S9. Antibody subclass-specific binding profiles in infection cohort participant #4. ....	23
Figure S10. Antibody subclass-specific binding profiles in infection cohort participant #5. ....	25
Figure S11. Multi-variable longitudinal profiling of Ig binding responses in response to seasonal Influenza vaccination. ....	27
Figure S12. Model for estimating protective Influenza responses according to HAI correlations. ....	29
Figure S13. Comparison of Ig binding responses against Influenza hemagglutinins included vs not included in the seasonal vaccine. ....	31
Figure S14. Anti-hemagglutinin Influenza responses by phylogenetic relatedness. ....	33
Figure S15. Vaccine-induced responses by antigen and study year. ....	35
Figure S16. Vaccination response dynamics by vaccination history. ....	37
Figure S17. Impact of vaccination history on antigen-specific Ig binding responses. ....	39
Figure S18. Serological imprinting by year of birth across multiple antigens and study years, shown as linear regressions. ....	41
Figure S19. Serological imprinting by year of birth, shown side-by-side comparing individuals born <1968 and $\geq$ 1968. ....	43
Figure S20. Correlation analysis of antigen-specific binding responses, clinical, and demographic information. ....	45
Figure S21. Principal component analysis (PCA) of multiplex binding responses. ....	47
Figure S22. PCA-based hierarchical clustering. ....	49
Figure S23. UV-inactivation of H5N1 mouse immune sera. ....	51

## Overview of Supplementary Information

### **1. Cohort, Antigens, and Sequence Information (Tables).**

Tables S1-S5

### **2. Epidemiologic and Phylogenetic Context.**

Figures S1-S2

### **3. Assay Development, Validation, and High-Throughput Design.**

Figures S3-S5

### **4. Detailed Infection Cohort Seroprofiles.**

Figures S6-S10

### **5. Vaccination Cohort: Longitudinal, Multidimensional Responses.**

Figures S11-S13, S15-S16

### **6. Serological Imprinting and Year-of-Birth Effects.**

Figures S13-S15, S18-S19

### **7. Data-Driven Clustering and Multivariate Structure.**

Figures S17, S20-S22

### **8. UV inactivation of H5N1 mouse immune sera - biosafety.**

Figure S23

## Supplemental Tables

### **Table S1. Influenza Vaccination cohort – Clinical and demographic information.**

See Excel file: *Table S1\_Vaccination cohort.xlsx*

### **Table S2. Influenza Infection cohort – Clinical and demographic information.**

See Excel file: *Table S2\_Infection cohort.xlsx*

### **Table S3. Antigen and bead information.**

See Excel file: *Table S3\_Antigen and bead information.xlsx*

**Table S4. Egg-adapted mutations in hemagglutinin antigens.**

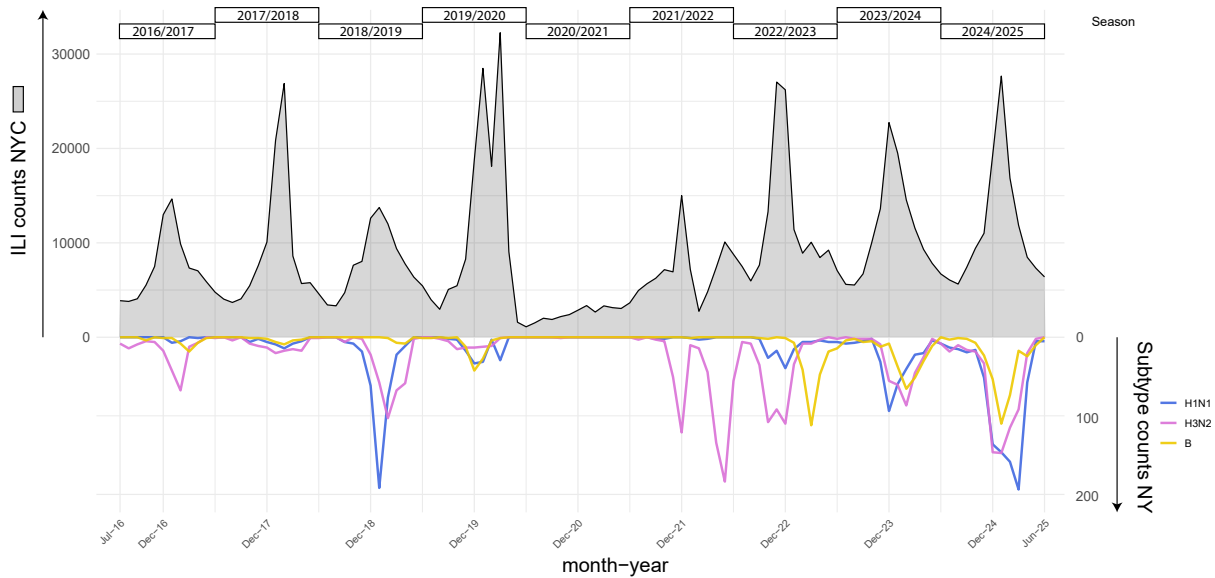
Antigens	Presence of egg-adapted mutations per (sub)type					
	H1: Q223R	H3: H156Q	H3: T160K	H3: L194P	B: G141R	B: N197D
A/bald/eagle/Florida/W22/134/OP/H5N1/HA 2022	-					
A/Brevig/Mission1/H1N1/HA/i 1918	-					
A/California/04/H1N1/HA/NonEggs 2009	-					
A/Japan/305/H2N2/HA/Eggs 1957	-					
A/Michigan/45/H1N1/HA 2015	YES					
A/Victoria/4897/H1N1/HA 2022	-					
A/Vietnam/1194/H5N1/HA/i 2004	-					
A/Wisconsin/588/H1N1/HA 2019	-					
A/Cambodia/e0826360/H3N2/HA 2020		-	-	-		
A/Darwin/9/H3N2/HA 2021		-	-	-		
A/HongKong/1/ACU79871/A/H3N2 1968		-	-	-		
A/Shanghai/1/H7N9/HA 2013		-	-	-		
B/Austria/1359417/Victoria/lineage/HA 2021					-	YES
B/Phuket/3073/Yamagata/lineage/HA 2013					-	-
B/Washington/02/Victoria/lineage/HA 2019					-	-

**Table S5. Linear and logistic regression data on binding responses by year of birth.**

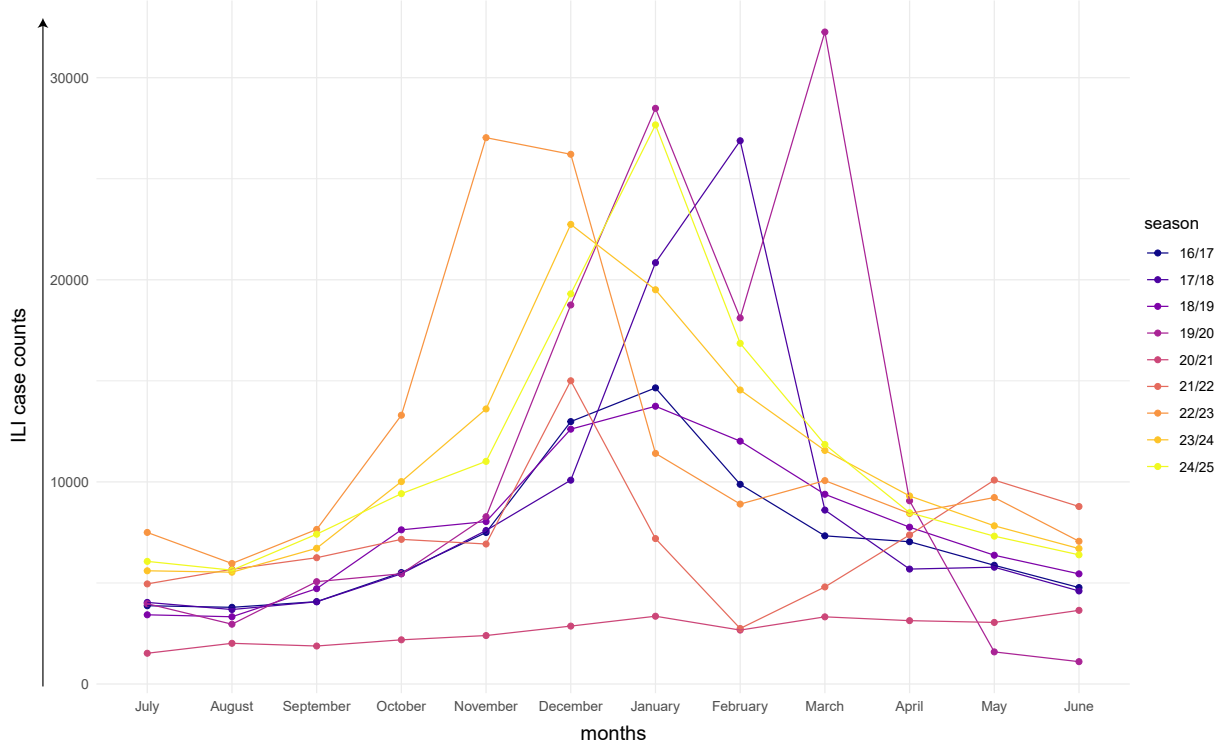
See Excel file: *Table S5\_Linear and logistic regression data.xlsx*

## Supplemental Figures

**A** Influenza-like illnesses (ILI) and Influenza subtypes in NY over the past 10 years



**B** ILI in NYC per season, overlay



**C** Vaccination strains per season over the past 10 years

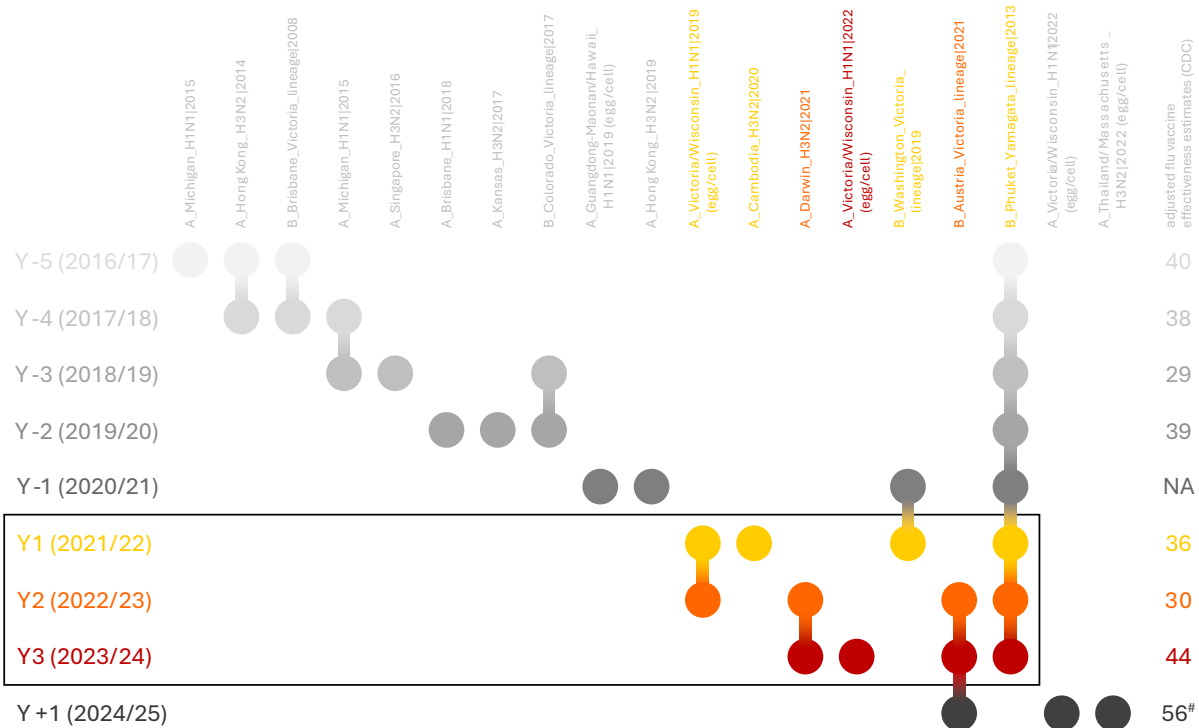


**Figure S1. Influenza-like illnesses (ILI), subtypes, and vaccine composition.**

**A.** Timeline of ILI cases in NYC (facing up; source: NYC.gov) and subtype counts in the state of New York (facing down; source: GISAIID) over the past ten years. **B.** Overlay of yearly ILI cases (from A) to compare seasonality and monthly ILI counts across the past ten years. **C.** Strain composition of quadri/tri-valent vaccines and their adjusted overall effectiveness per year (%). Study years are highlighted. Source: CDC.gov/flu-vaccines-work, #preliminary data.

Timescale (years)

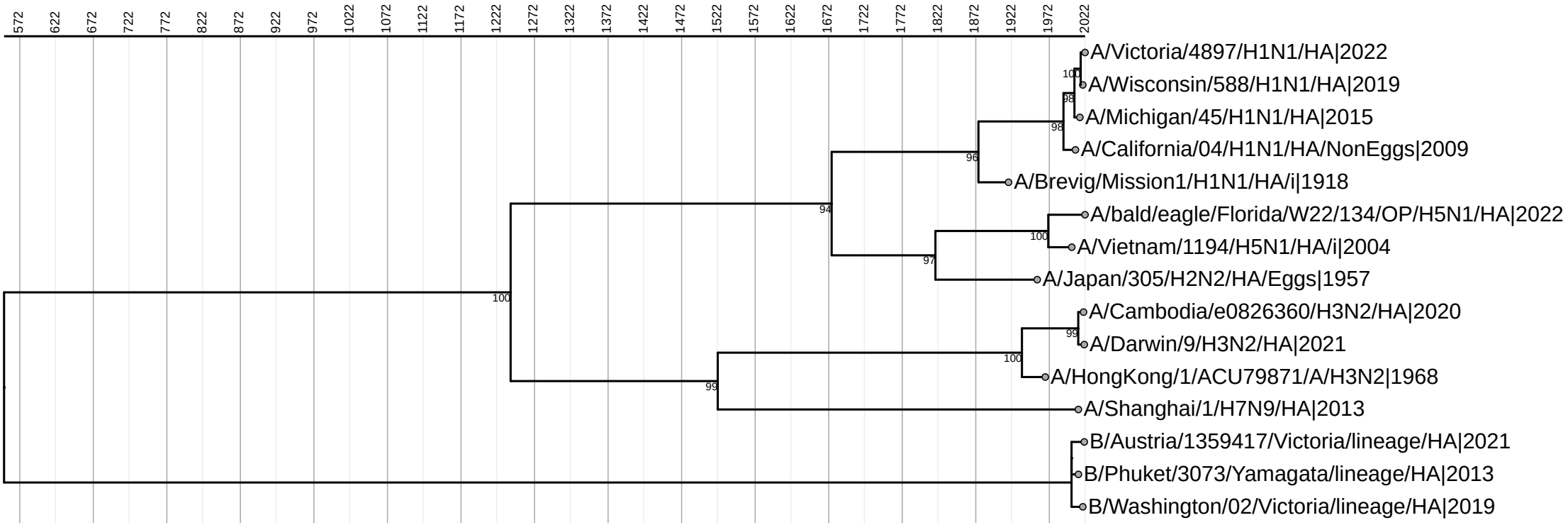
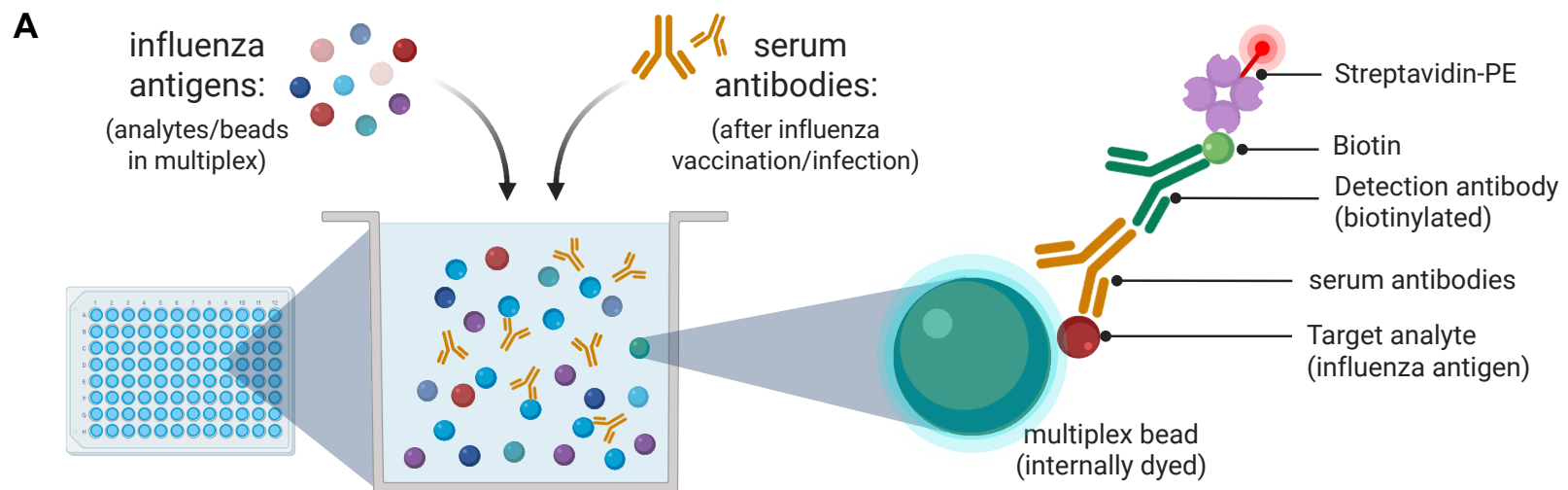
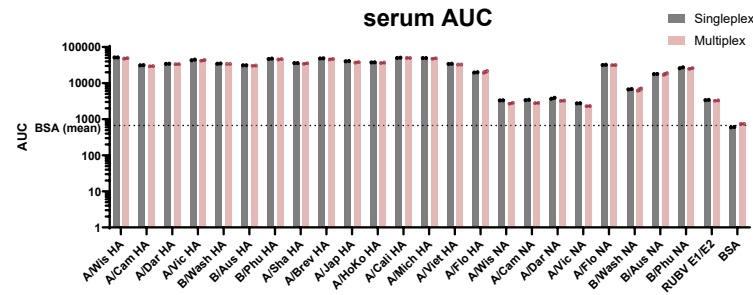


**Figure S2. Phylogenetic relatedness of used hemagglutinin antigens.**

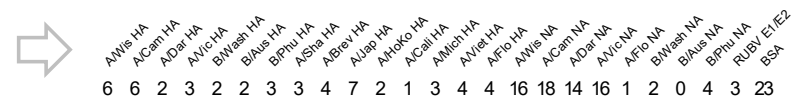
**B.** Time-calibrated global tree using sequences of the studied HA antigens across (sub)types and groups (IQ tree, 1,000 bootstrap replicates). Bootstrap values > 70 are indicated.



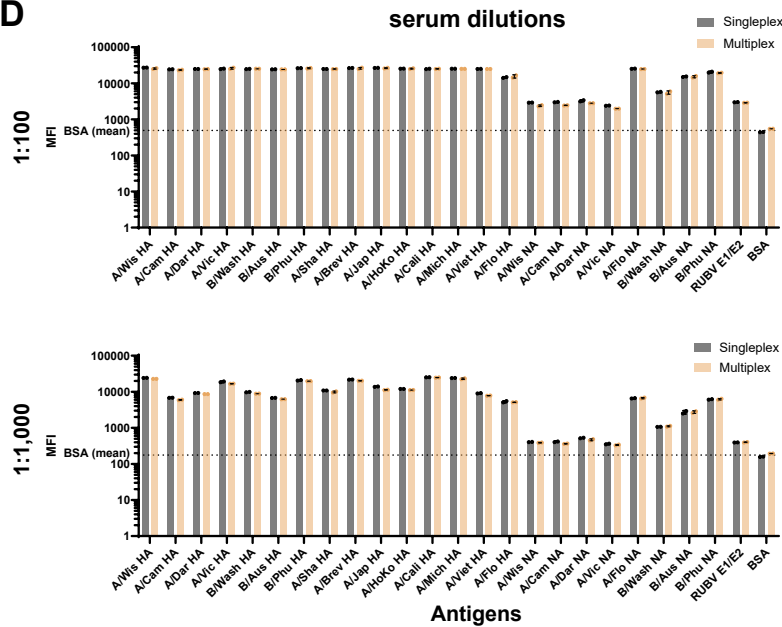
**B** single vs multiplex



**C** Variance (%) - single vs multiplex



**D**



**E**

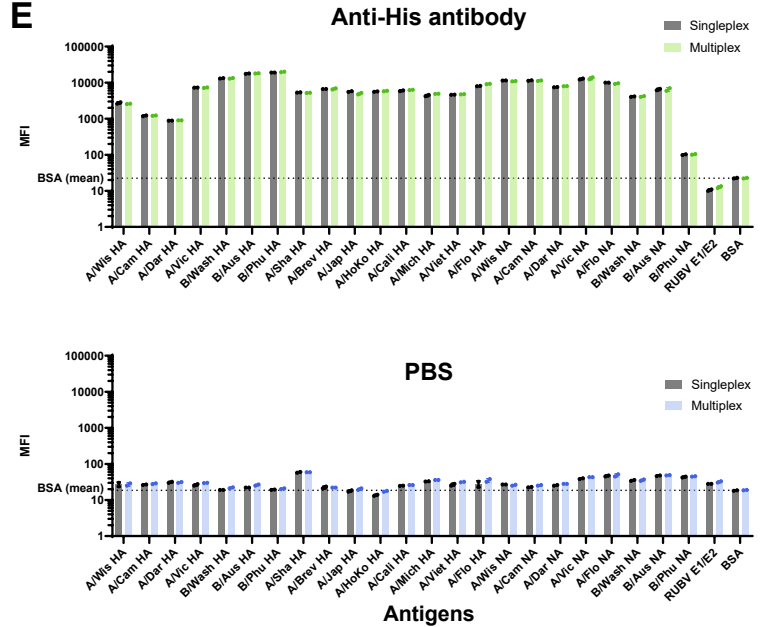
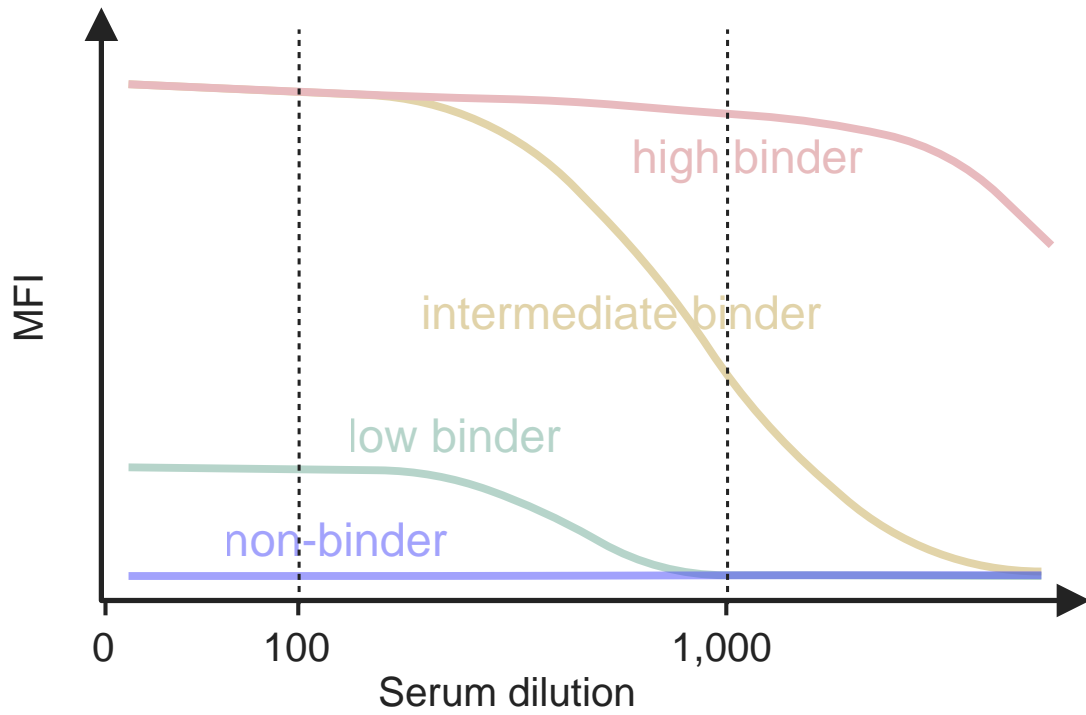


**Figure S3. Comparability of signals obtained in multiplex versus singleplex.**

To verify the absence of significant cross-competition among antigens in the multiplex format, we compared total Ig signals obtained with the positive control serum in the multiplex (multiple Influenza antigens run simultaneously) with those in the singleplex format (only one Influenza antigen measured at a time). Each Influenza singleplex was run with BSA and IC45 controls included, and was technically a triplex. **A.** Schematic setup of multiplex bead-based binding assay (MBA). **B.** Signal comparison for area under the curve (AUC) measurements. **C.** Variance between multiplex and singleplex in B:  $([\text{multiplex} - \text{singleplex}]/\text{singleplex}) * 100\%$ . **D.** Comparison as in B, but with individual dilutions measured in median fluorescence intensities (MFI; raw values). **D.** Additional controls, i.e., using PBS (bottom) instead of the positive control serum, and using anti-His antibody (1:2,000, top) instead of the positive control serum and Ig detection antibody. The dashed line indicates the averaged binding responses against BSA as a reference.

### A Two serum-dilution strategy



### B Simplified AUC

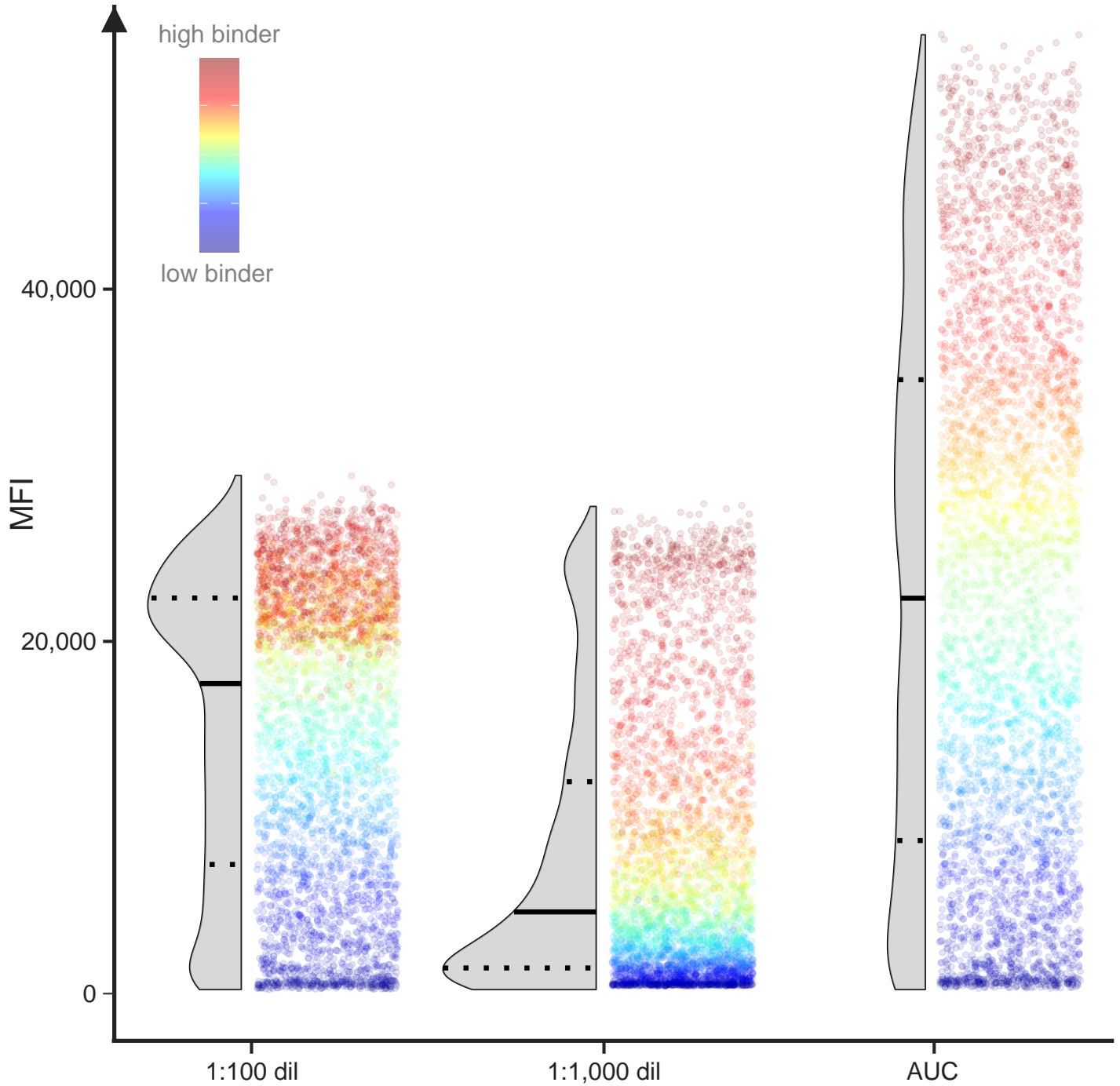
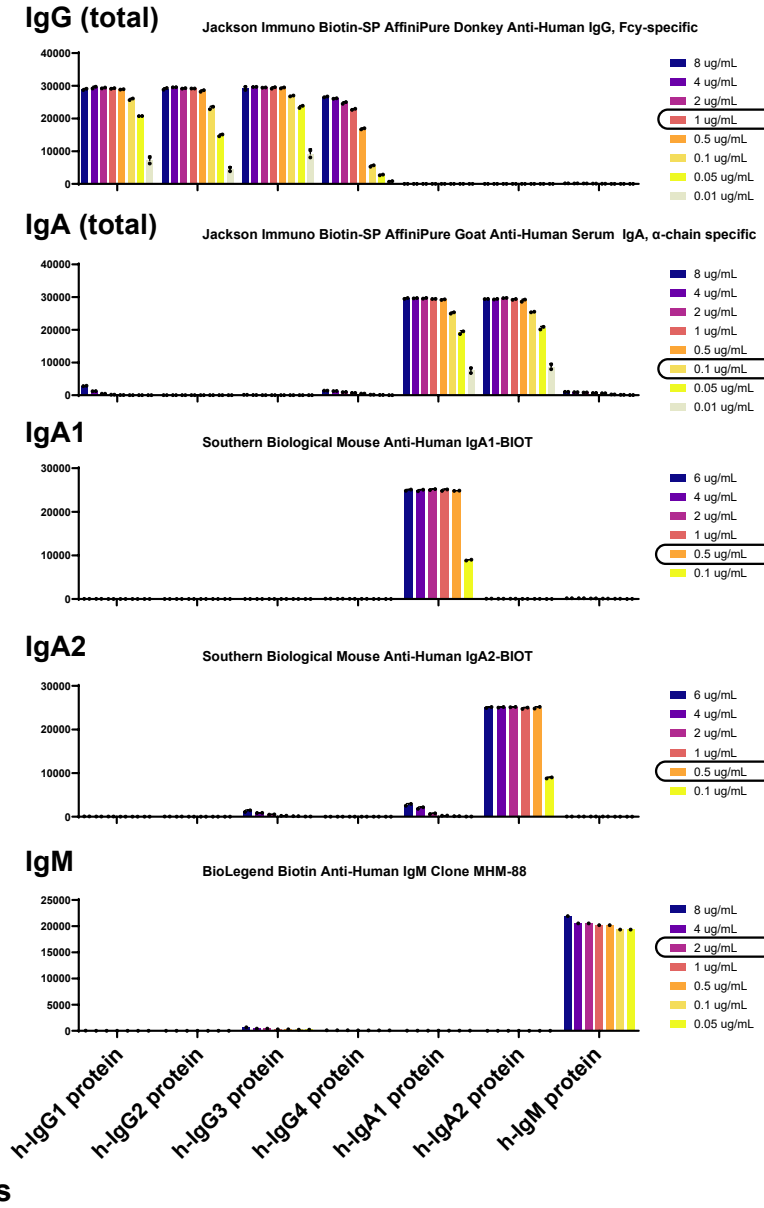
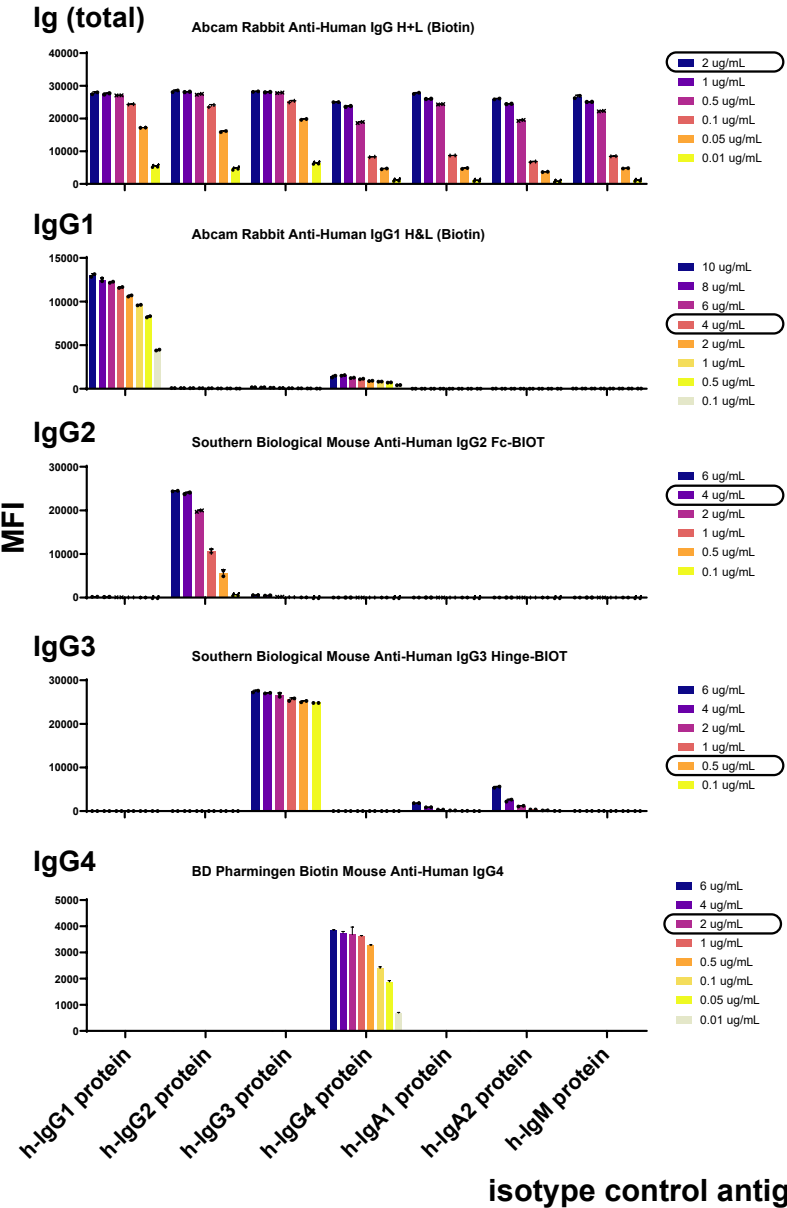


**Figure S4. Two-Serum Dilution Strategy for high-throughput immunoprofiling with high resolution.**

**A.** Schematic representation of antigen-specific IgG titration curves observed in a human vaccination or infection study cohort. Examples include participants categorized as non-binders, low binders, intermediate binders, and high binders. **B.** Distribution of antigen-specific IgG levels measured at two distinct serum dilutions or represented as a simplified AUC (area under the curve), calculated by summing both measurements per data point (n=3956 data points, vaccination cohort of 30 participants: 172 visits, 23 Influenza antigens).

# A Isotype and subclass detection antibodies - titration, sensitivity and specificity



# B Relative binding

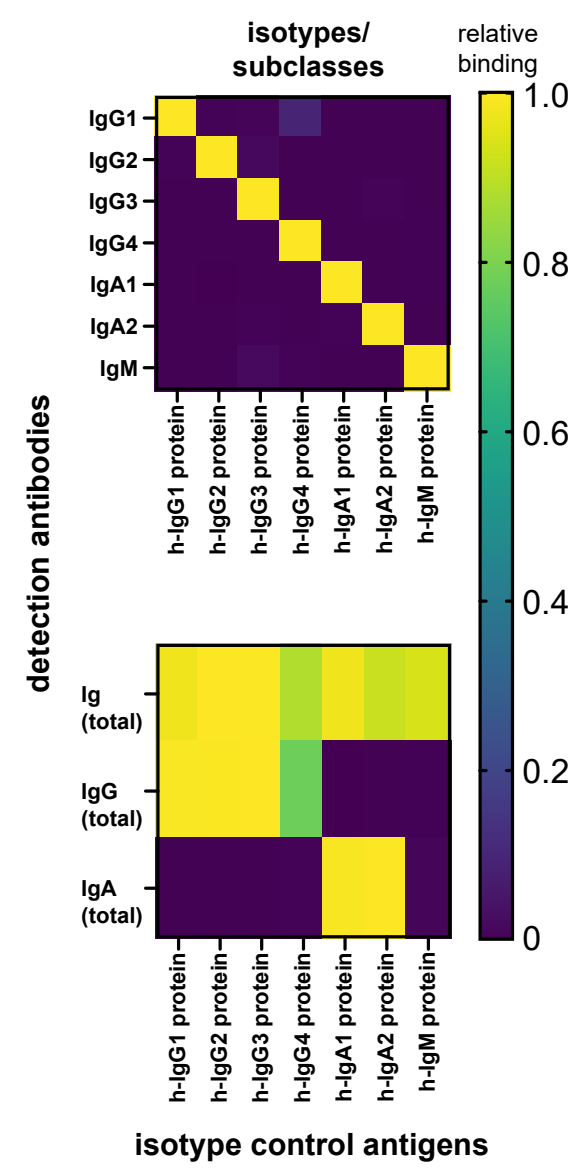
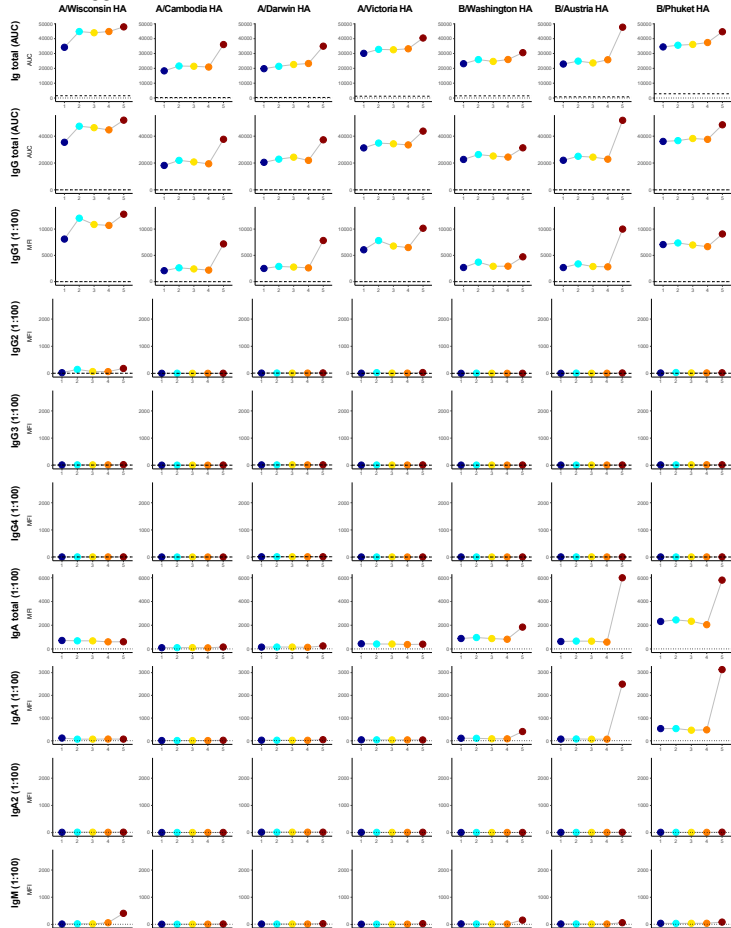


**Figure S5. Development and optimization of an Ig isotype and subclass-specific binding assay.**

**A.** Titration of indicated Ig, IgG, IgA, and IgM isotype and subclass antibodies against isotype/subclass control antigens. The antibody concentrations selected for the main experiments are encircled. **B.** Heatmaps to highlight the specificity of the antibodies.

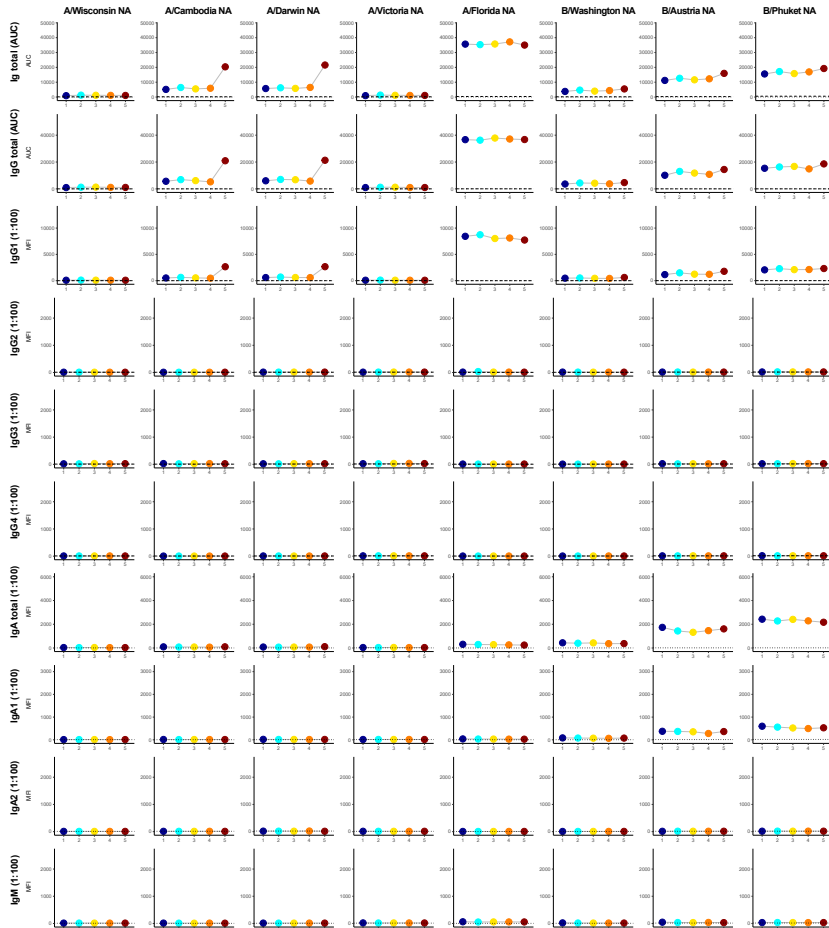
### A Hemagglutinin - recent vaccine strains



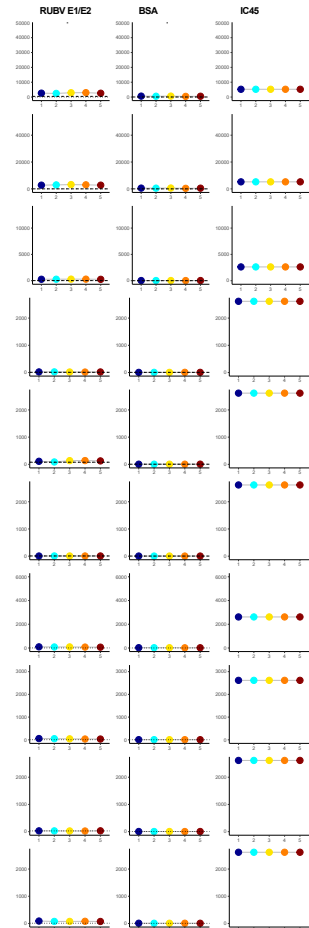
### B Hemagglutinin - historic/pandemic potential



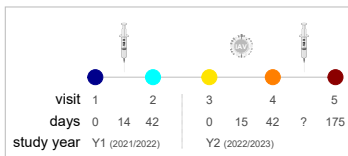
### C Neuraminidase



### D Controls



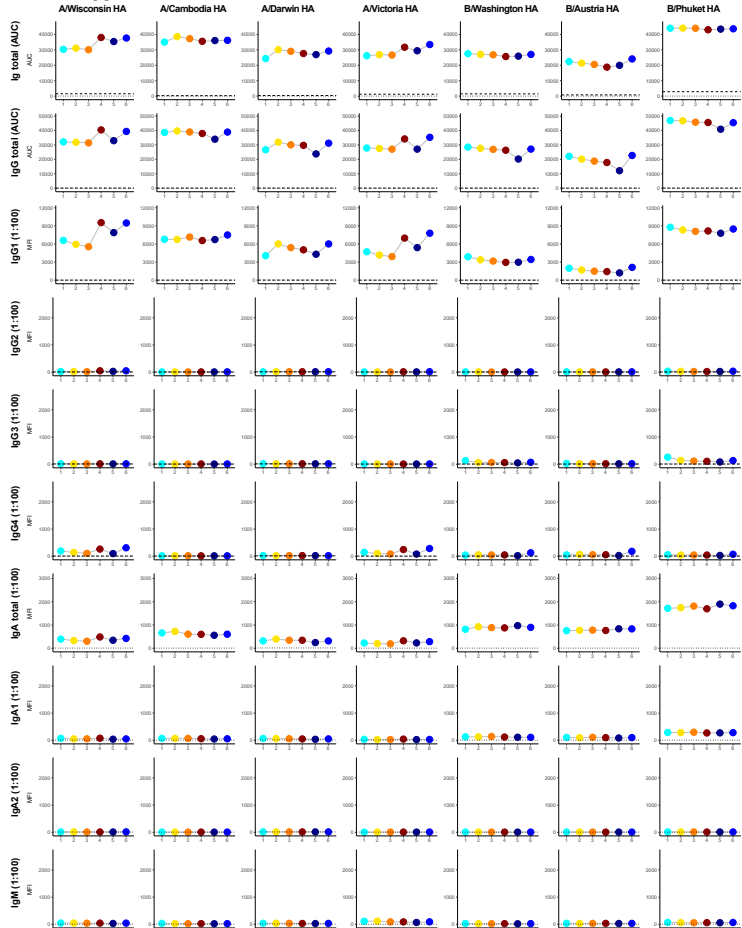
#Inf\_1



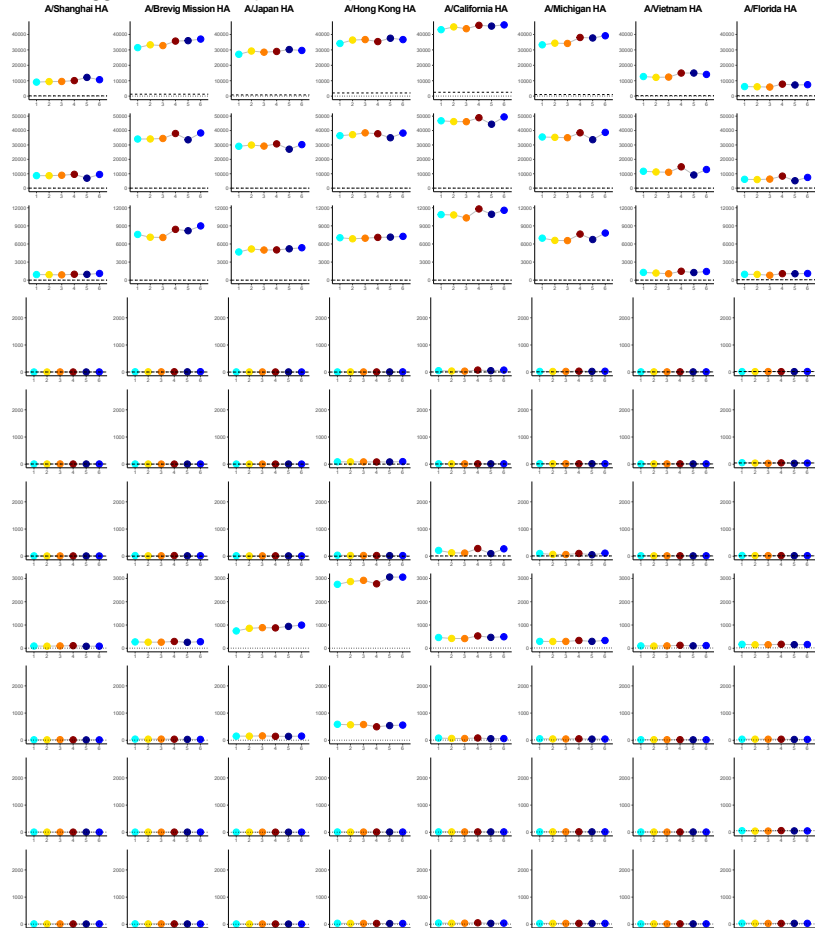
----- IgG-depleted serum (neg. control)  
 ..... PBS (neg. control)

**Figure S6. Antibody subclass-specific binding profiles in infection cohort participant #1.** Longitudinal multi-isotype and -subclass anti-Influenza profiling against the 26-plex antigens/beads, including 15 hemagglutinins (**A**, **B**), 8 neuraminidases (**C**), and three controls (**D**). The timeline of longitudinal samplings, vaccinations, and infection is shown in the box. Antibody binding levels in MFI using 1:100 serum dilution or AUC (for total Ig and IgG) are shown where the dashed line indicates IgG-depleted serum control and the dotted line PBS (run in single measurements). AUC: area under the curve, MFI: median fluorescence intensity.

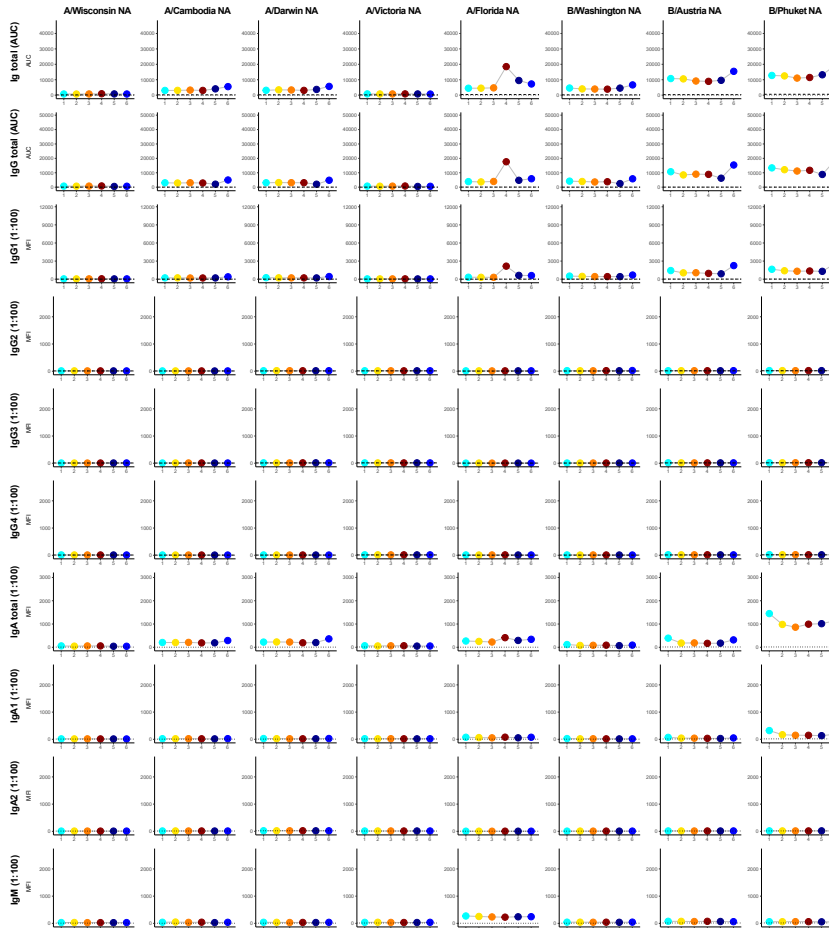
### A Hemagglutinin - recent vaccine strains



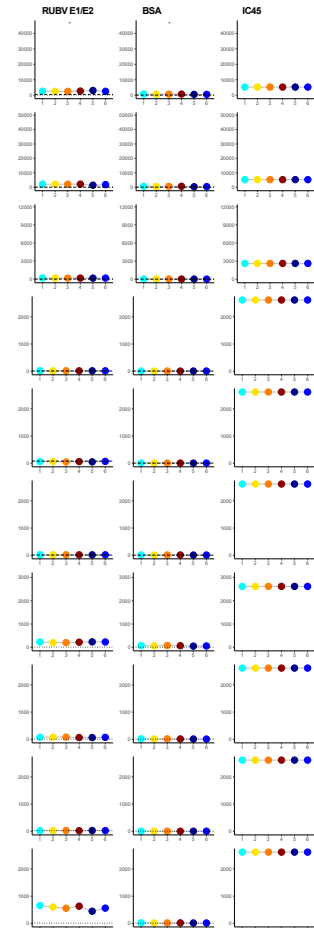
### B Hemagglutinin - historic/pandemic potential



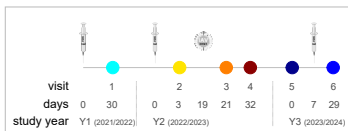
### C Neuraminidase



### D Controls



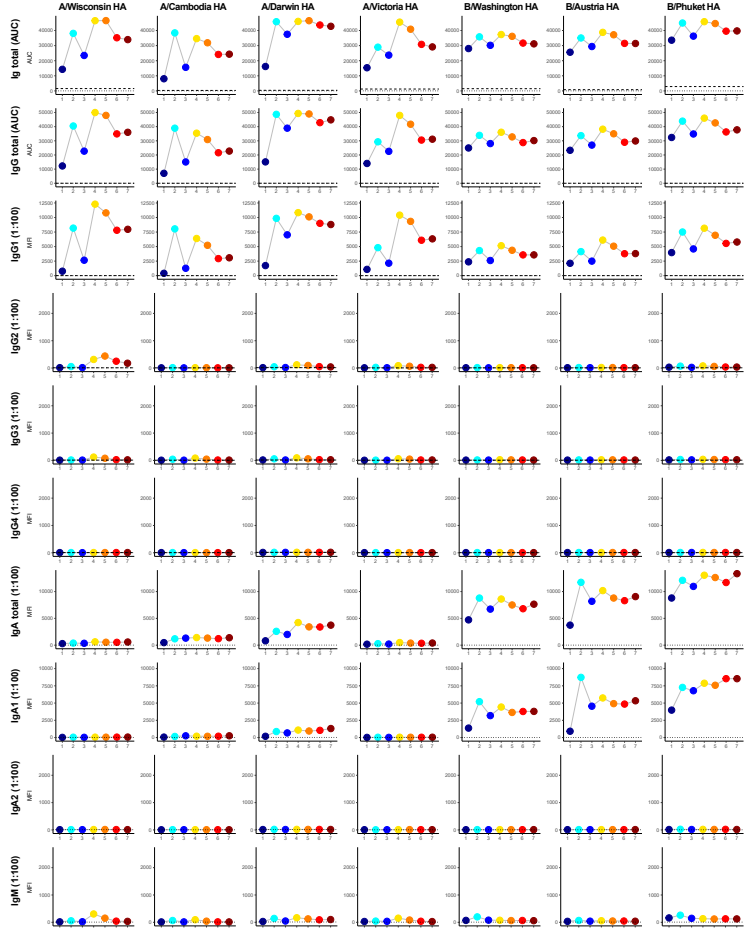
#Inf\_2



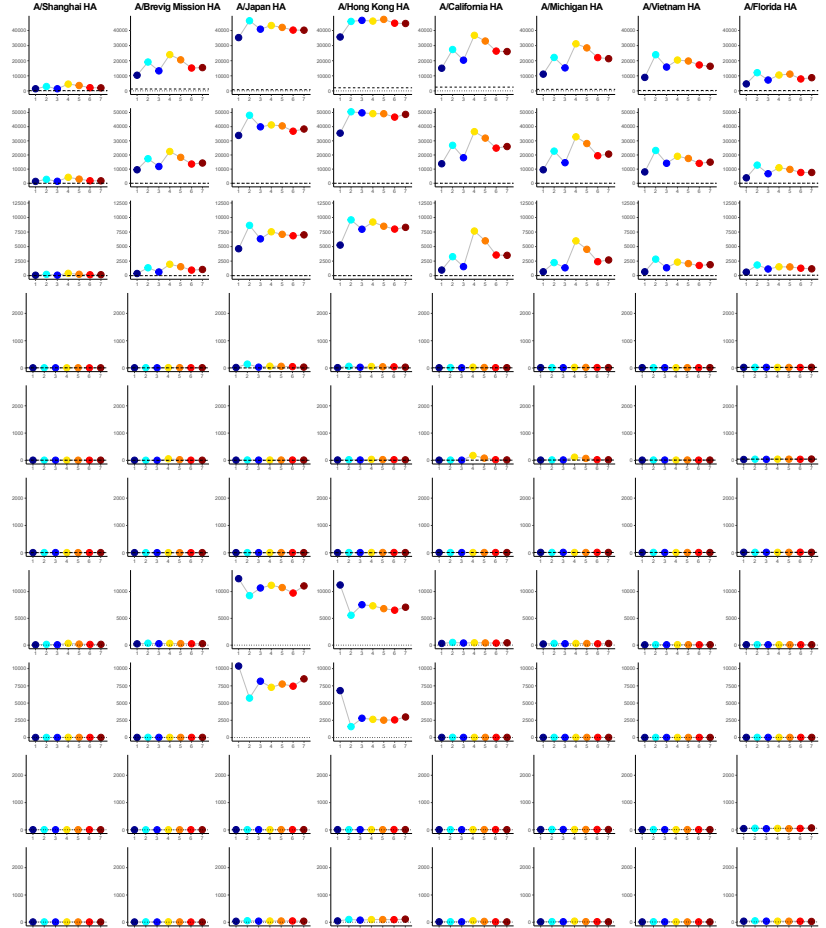
----- IgG-depleted serum (neg. control)  
 ..... PBS (neg. control)

**Figure S7. Antibody subclass-specific binding profiles in infection cohort participant #2.** Longitudinal multi-isotype and -subclass anti-Influenza profiling against the 26-plex antigens/beads, including 15 hemagglutinins (**A**, **B**), 8 neuraminidases (**C**), and three controls (**D**). The timeline of longitudinal samplings, vaccinations, and infection is shown in the box. Antibody binding levels in MFI using 1:100 serum dilution or AUC (for total Ig and IgG) are shown where the dashed line indicates IgG-depleted serum control and the dotted line PBS (run in single measurements). AUC: area under the curve, MFI: median fluorescence intensity.

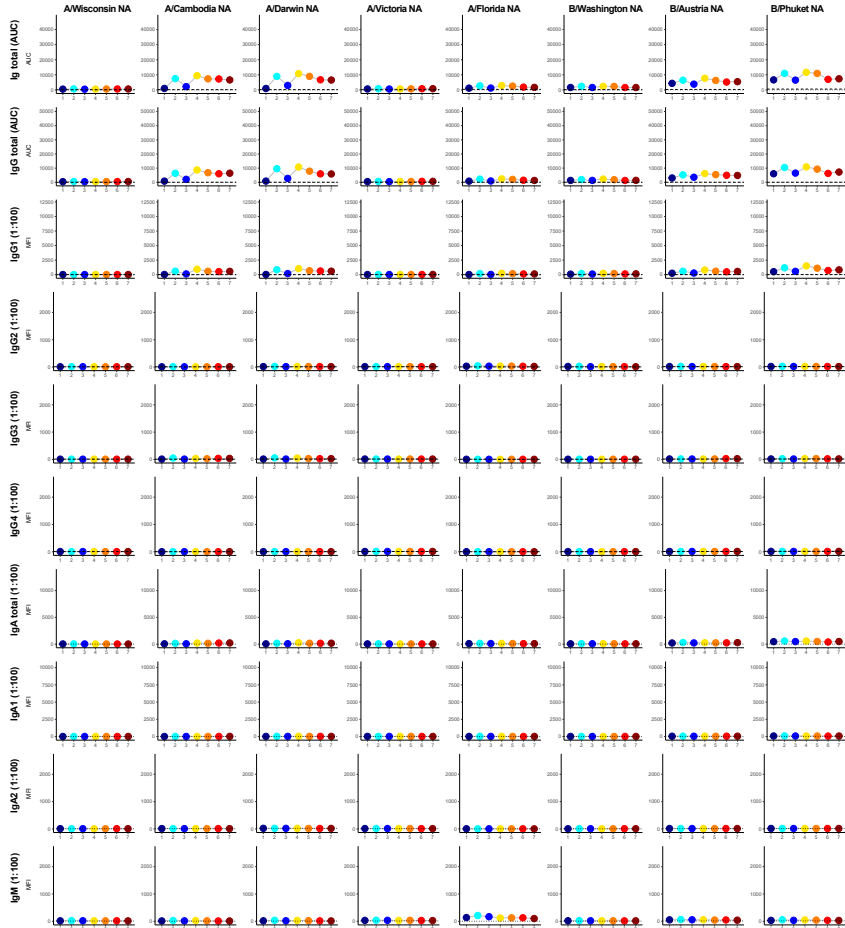
### A Hemagglutinin - recent vaccine strains



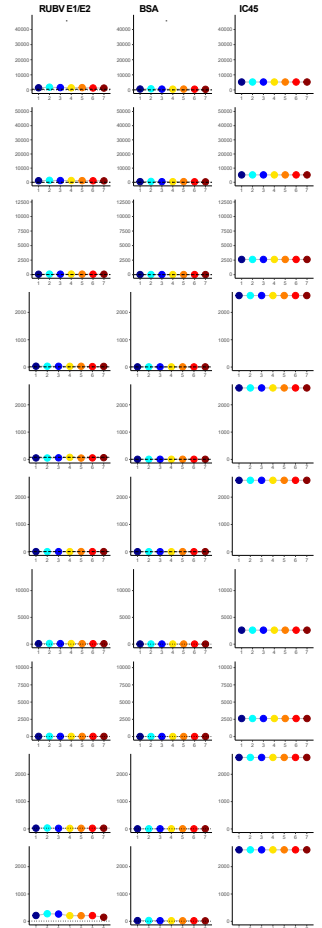
### B Hemagglutinin - historic/pandemic potential



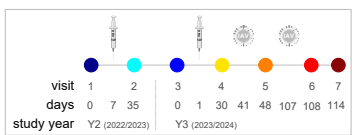
### C Neuraminidase



### D Controls



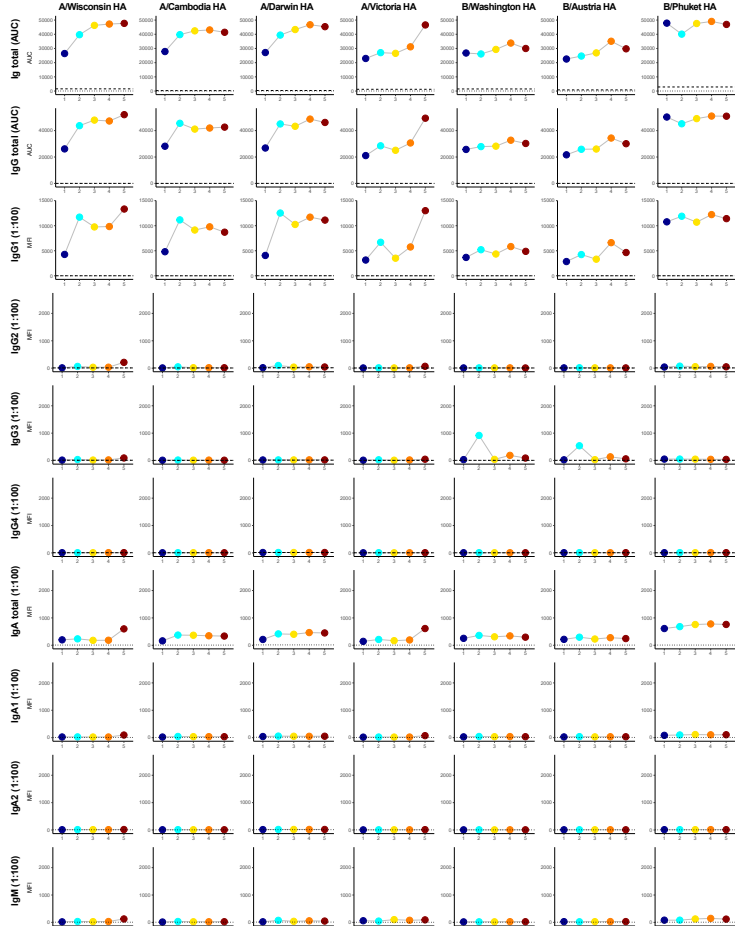
#Inf\_3



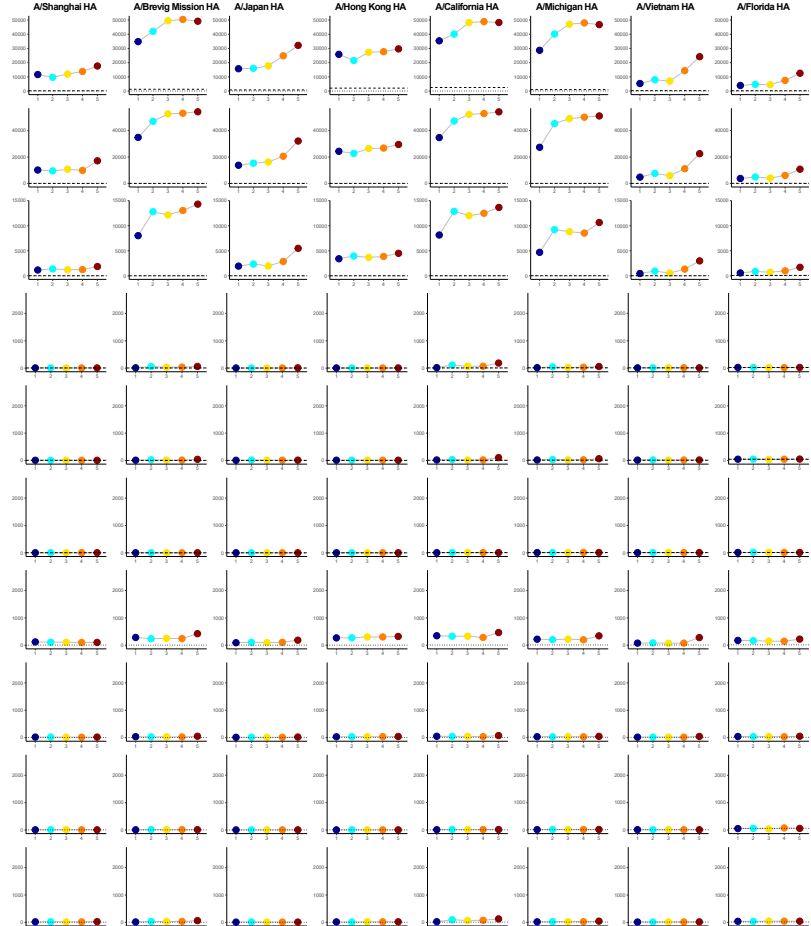
--- IgG-depleted serum (neg. control)  
 ..... PBS (neg. control)

**Figure S8. Antibody subclass-specific binding profiles in infection cohort participant #3.** Longitudinal multi-isotype and -subclass anti-Influenza profiling against the 26-plex antigens/beads, including 15 hemagglutinins (**A**, **B**), 8 neuraminidases (**C**), and three controls (**D**). The timeline of longitudinal samplings, vaccinations, and infections is shown in the box. Antibody binding levels in MFI using 1:100 serum dilution or AUC (for total Ig and IgG) are shown where the dashed line indicates IgG-depleted serum control and the dotted line PBS (run in single measurements). AUC: area under the curve, MFI: median fluorescence intensity.

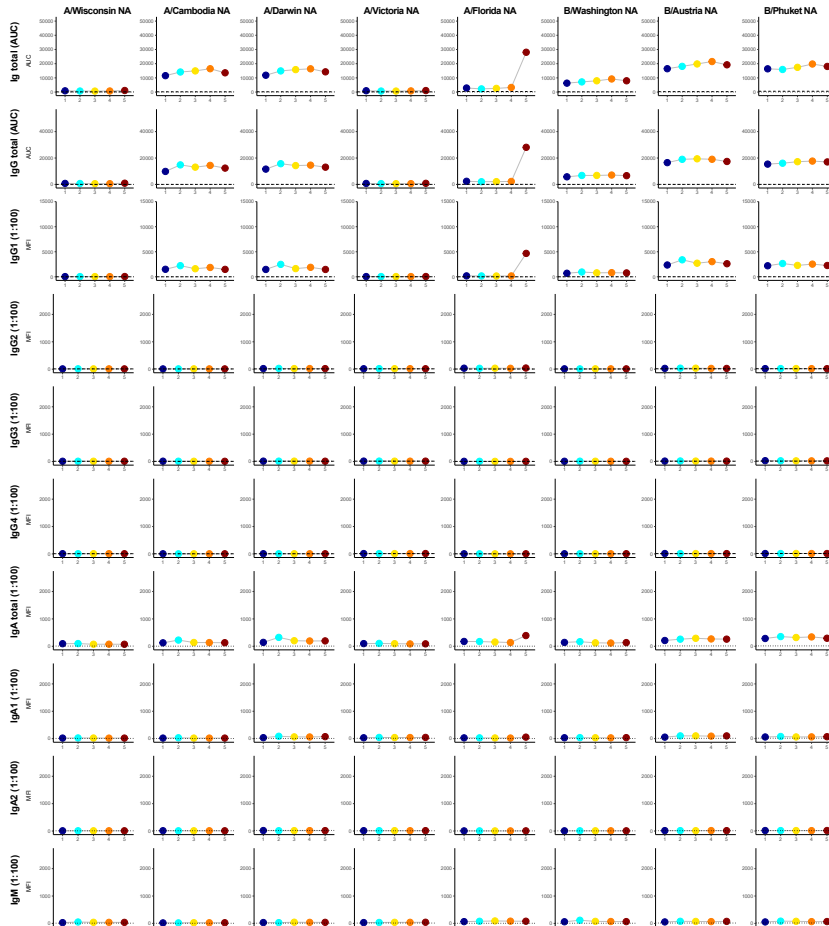
### A Hemagglutinin - recent vaccine strains



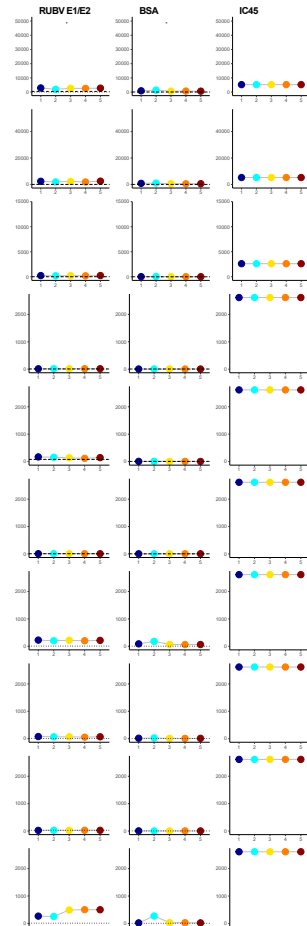
### B Hemagglutinin - historic/pandemic potential



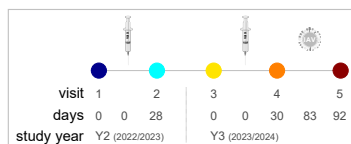
### C Neuraminidase



### D Controls



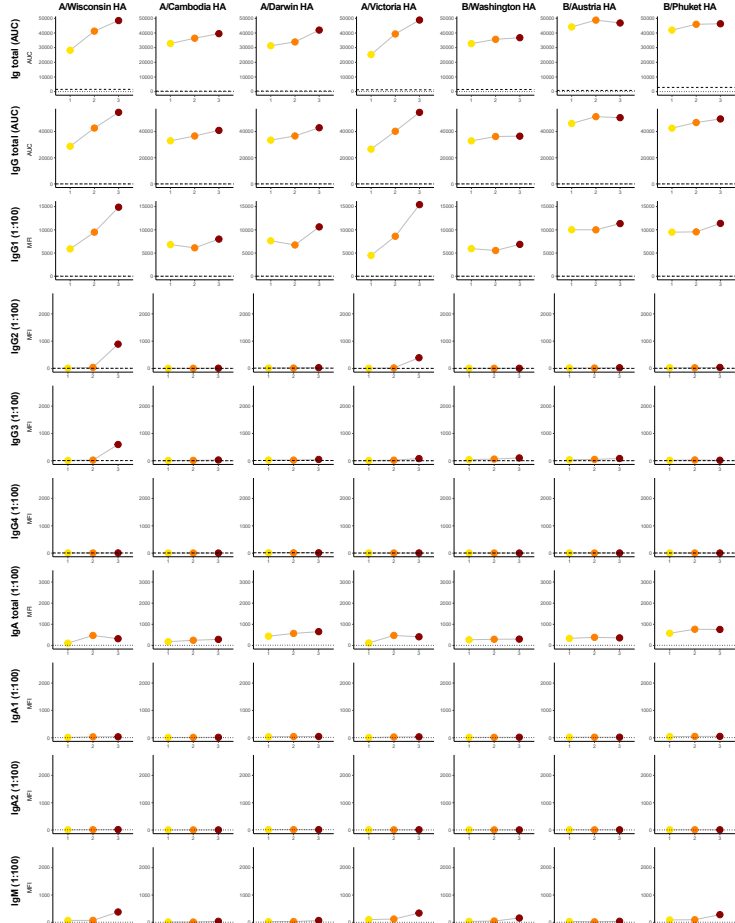
#Inf\_4



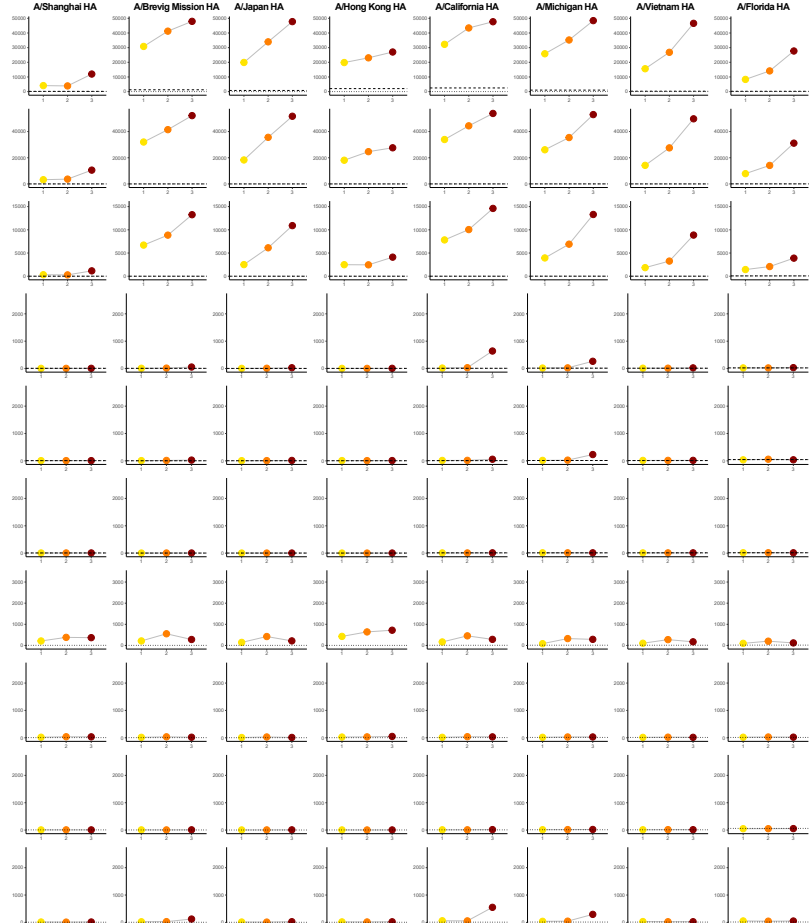
----- IgG-depleted serum (neg. control)  
 ..... PBS (neg. control)

**Figure S9. Antibody subclass-specific binding profiles in infection cohort participant #4.** Longitudinal multi-isotype and -subclass anti-Influenza profiling against the 26-plex antigens/beads, including 15 hemagglutinins (**A**, **B**), 8 neuraminidases (**C**), and three controls (**D**). The timeline of longitudinal samplings, vaccinations, and infection is shown in the box. Antibody binding levels in MFI using 1:100 serum dilution or AUC (for total Ig and IgG) are shown where the dashed line indicates IgG-depleted serum control and the dotted line PBS (run in single measurements). AUC: area under the curve, MFI: median fluorescence intensity.

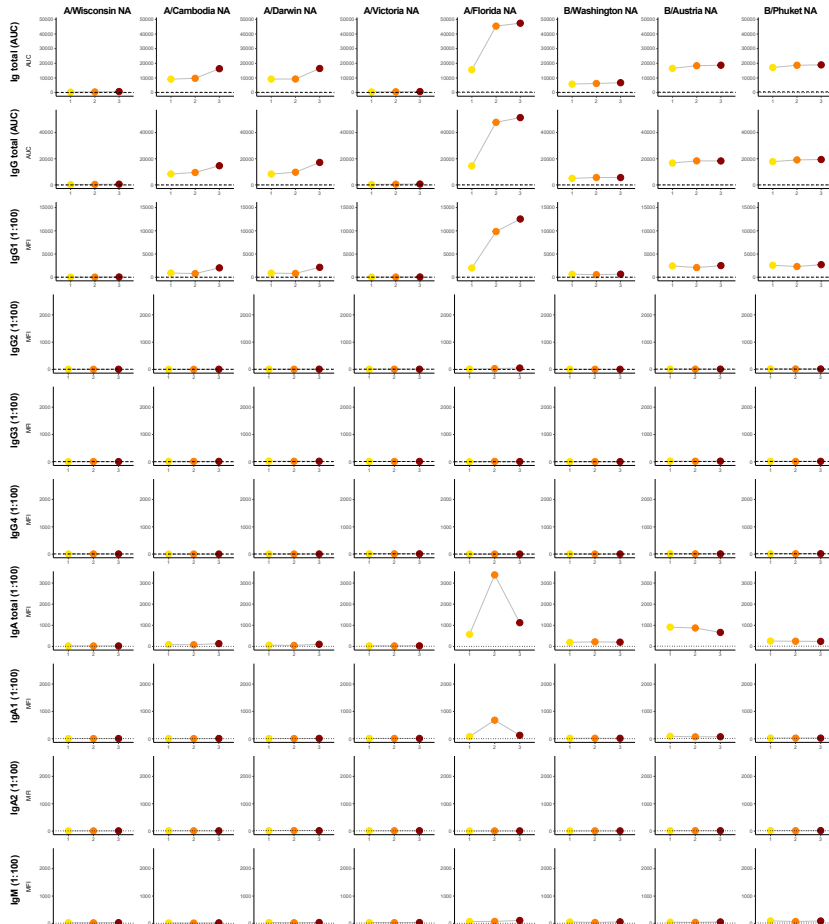
### A Hemagglutinin - recent vaccine strains



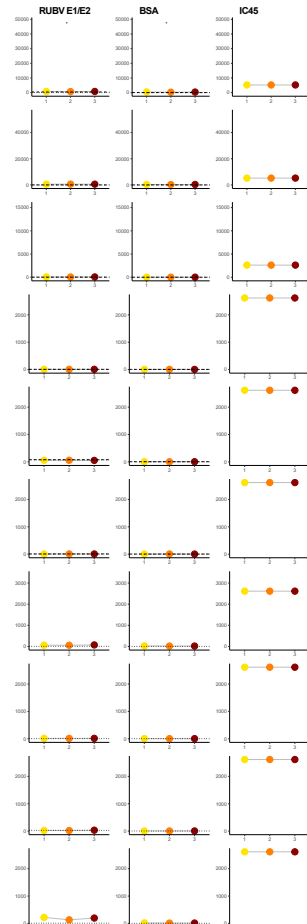
### B Hemagglutinin - historic/pandemic potential



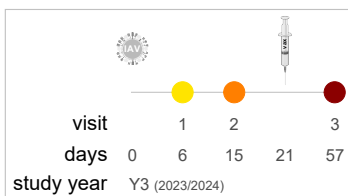
### C Neuraminidase



### D Controls



#Inf\_5



----- IgG-depleted serum (neg. control)  
 ..... PBS (neg. control)

**Figure S10. Antibody subclass-specific binding profiles in infection cohort participant #5.** Longitudinal multi-isotype and -subclass anti-Influenza profiling against the 26-plex antigens/beads, including 15 hemagglutinins (**A**, **B**), 8 neuraminidases (**C**), and three controls (**D**). The timeline of longitudinal samplings, vaccinations, and infection is shown in the box. Antibody binding levels in MFI using 1:100 serum dilution or AUC (for total Ig and IgG) are shown where the dashed line indicates IgG-depleted serum control and the dotted line PBS (run in single measurements). AUC: area under the curve, MFI: median fluorescence intensity.

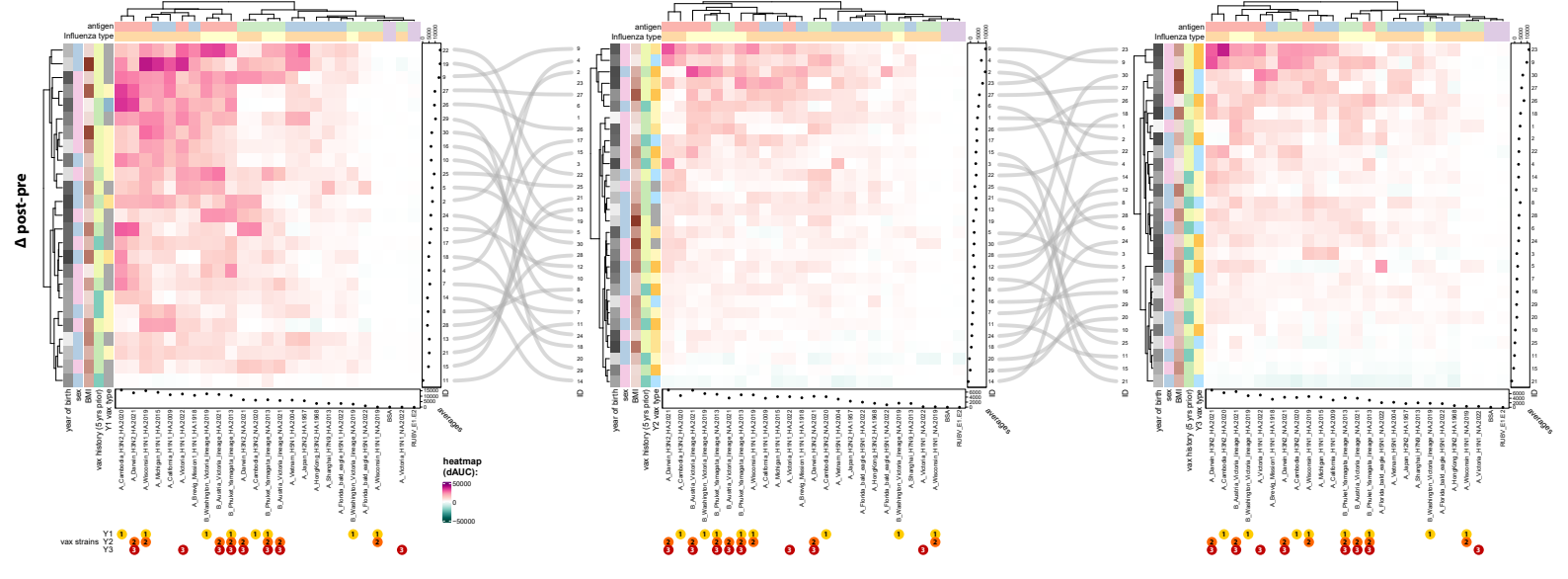
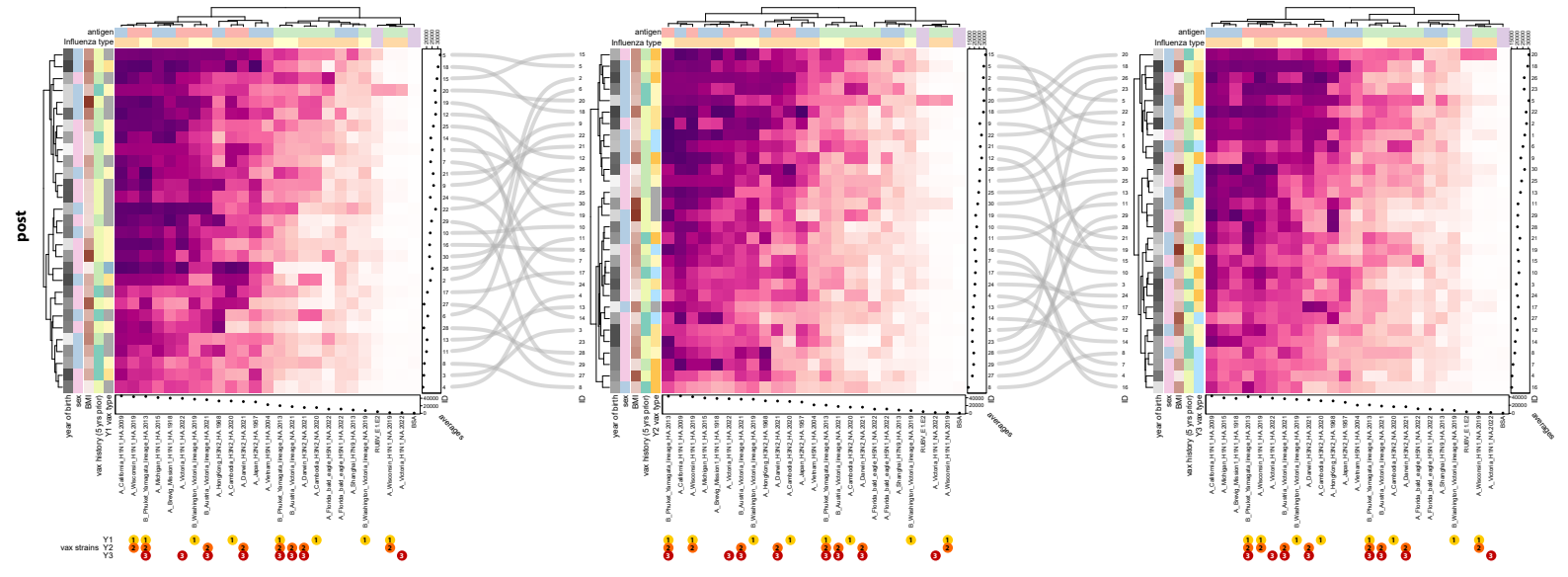
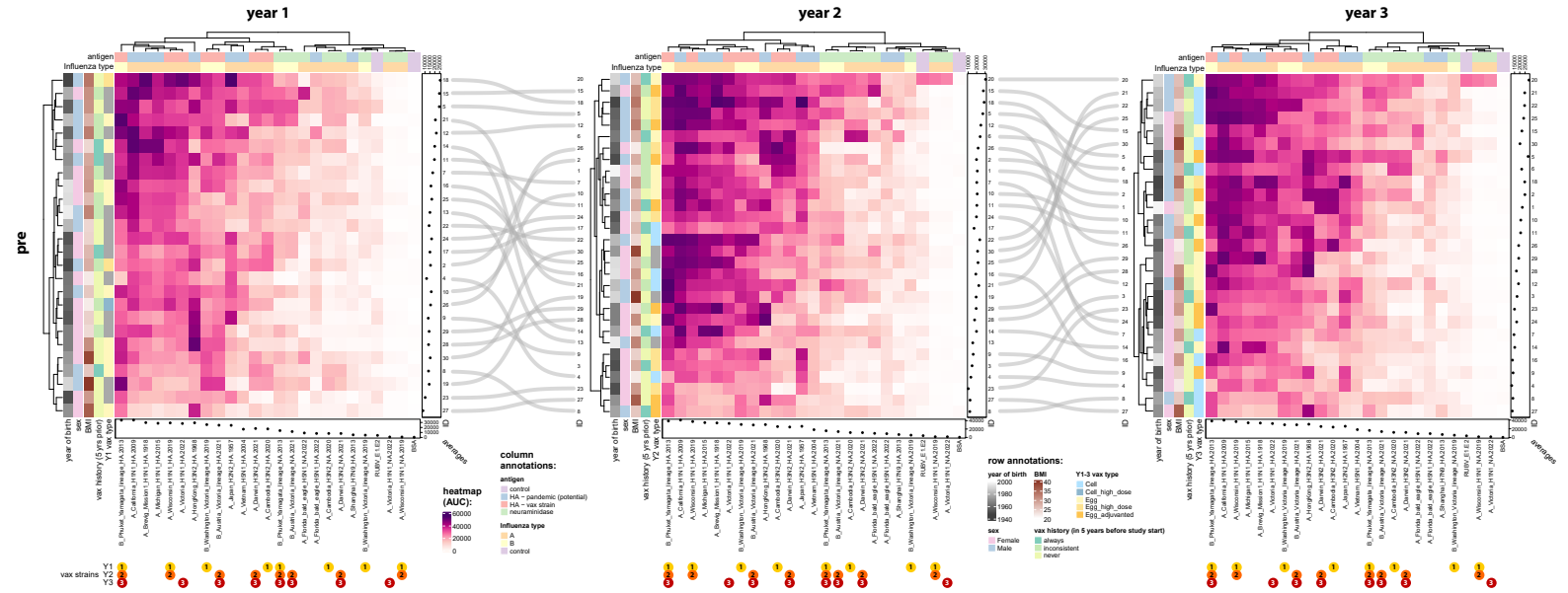
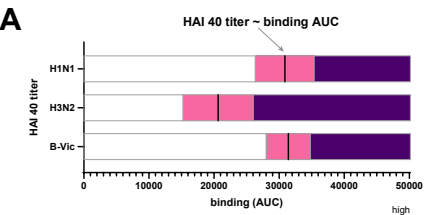


**Figure S11. Multi-variable longitudinal profiling of Ig binding responses in response to seasonal Influenza vaccination.**

Heatmaps of Ig binding profiles for 30 study participants against the 26-plex antigen/bead panel. Antibody levels are shown before (top row), approximately one month after vaccination (middle row), and for the vaccine-induced response (difference between pre- and post-vaccination; bottom row) across the three study years (left to right). The curved lines connecting the heatmaps enable track participants across years. Additional antigen and participant information are annotated above and to the left of each heatmap. Details about which antigens were included in the seasonal vaccines for the three study years are provided at the bottom of each heatmap.

**A**



H1N1: HAI 40 titer ~ 30,892 AUC (95% CI: 26,403 - 35,381 AUC) --> A/group1 (H1, H2, H5)  
 H3N2: HAI 40 titer ~ 20,622 AUC (95% CI: 15,254 - 25,998 AUC) --> A/group2 (H3, H7)  
 B-Vic: HAI 40 titer ~ 31,411 AUC (95% CI: 28,067 - 34,756 AUC) --> B

**row annotations:**

- year of birth: 1950, 1960, 1970, 1980, 1990, 2000
- sex: Female, Male
- vax history (in 5 years before study start): always, post-vaccinant, never
- Y1-3 vax type: Egg, Cell, High\_dose

**column annotations:**

- antigen: HA - pandemic (potential), HA - vax strain
- Influenza type: A, B

**B**

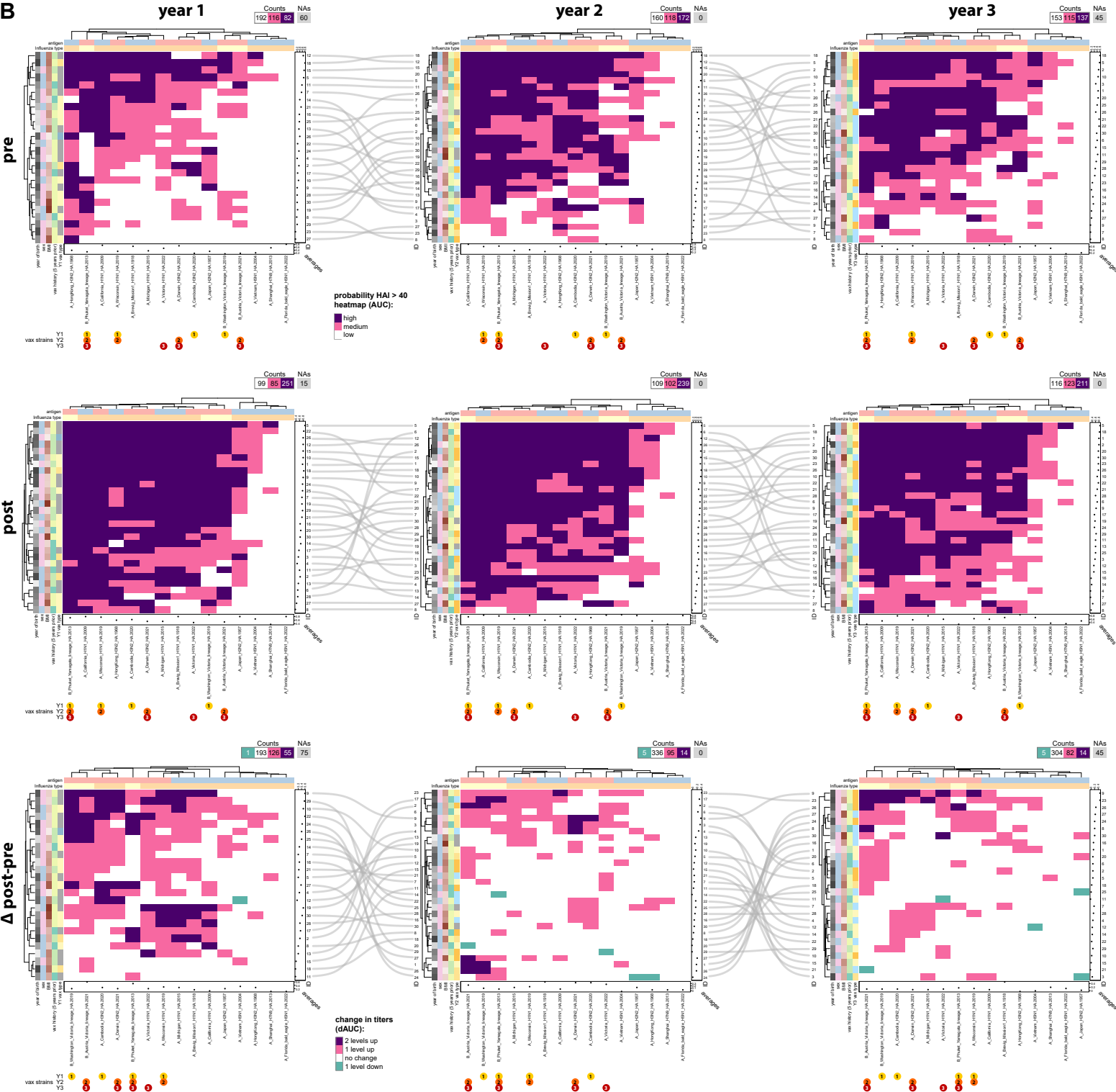


**Figure S12. Model for estimating protective Influenza responses according to HAI correlations.**

**A.** Linear mixed models using data from Figure 3 to interpolate binding levels correlating with HAI 40 titers including 95% confidence intervals (CI), for Influenza type A group 1, 2, and type B hemagglutinin responses. Values >95% CI are considered highly probable to have HAI > 40 titers and protective against related viruses. **B.** Heatmaps as in **Figure S12** applying color-coding as in **A** per Influenza type and group and focusing on hemagglutinin responses only. Counts of responses in the respective categories are shown on the top right for each heatmap. Unavailable data points (NAs), i.e., missed participant visits, are counted but not shown in heatmaps (empty rows).

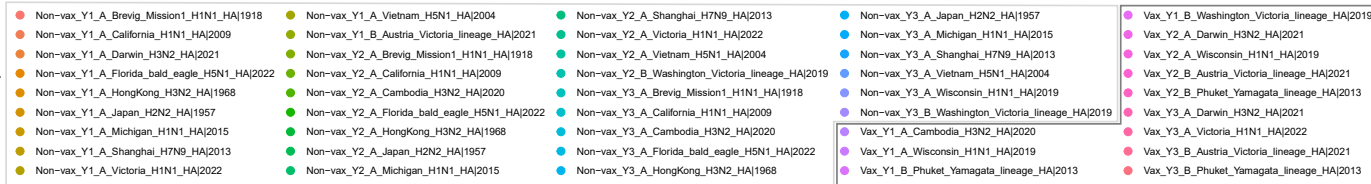
non-vax

vax

non-vax vax

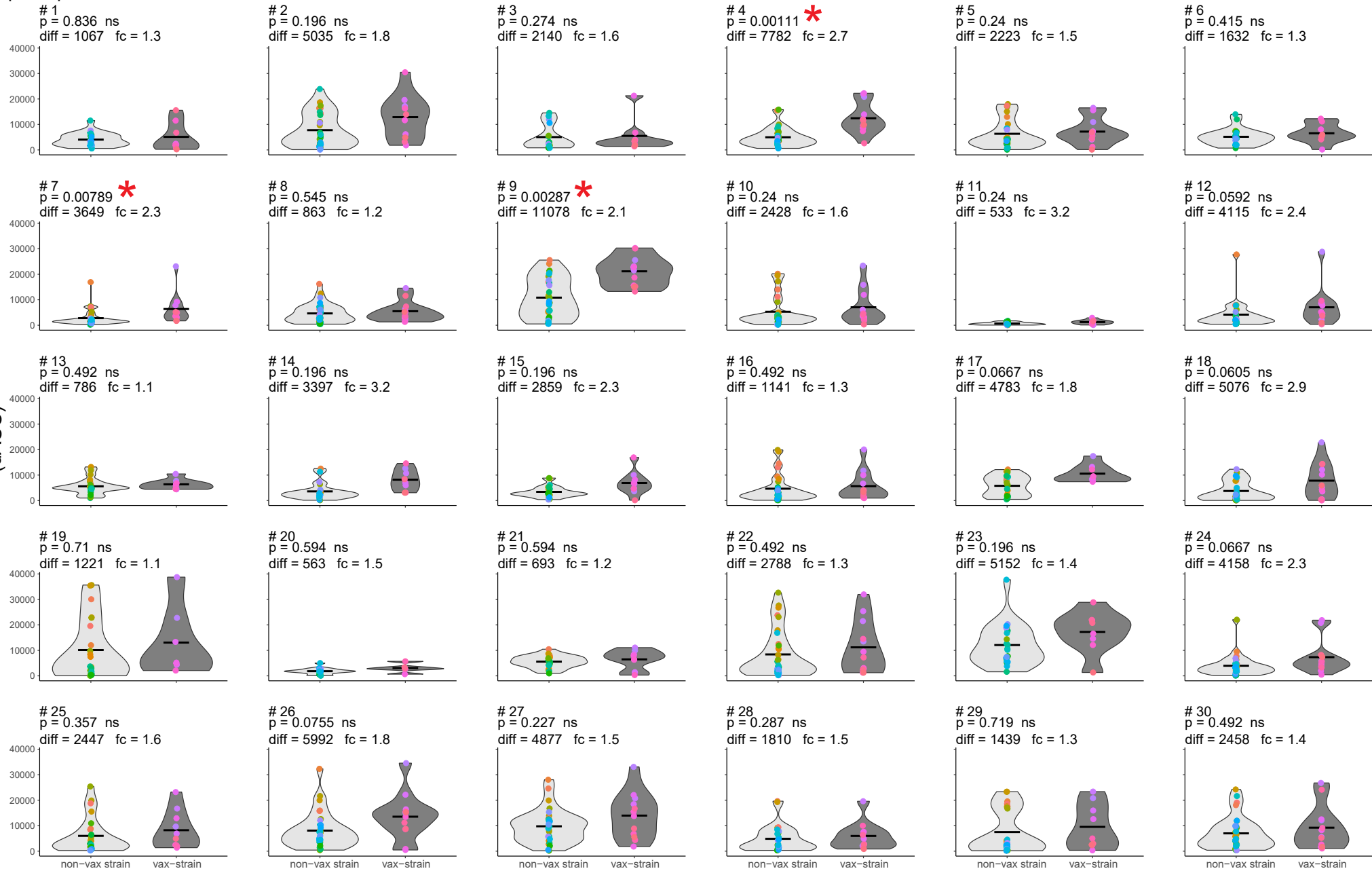


strain & year  
(vax/non-vax)



participants 1 - 30:

vaccine-induced responses,  $\Delta V1V2$   
(dAUC)

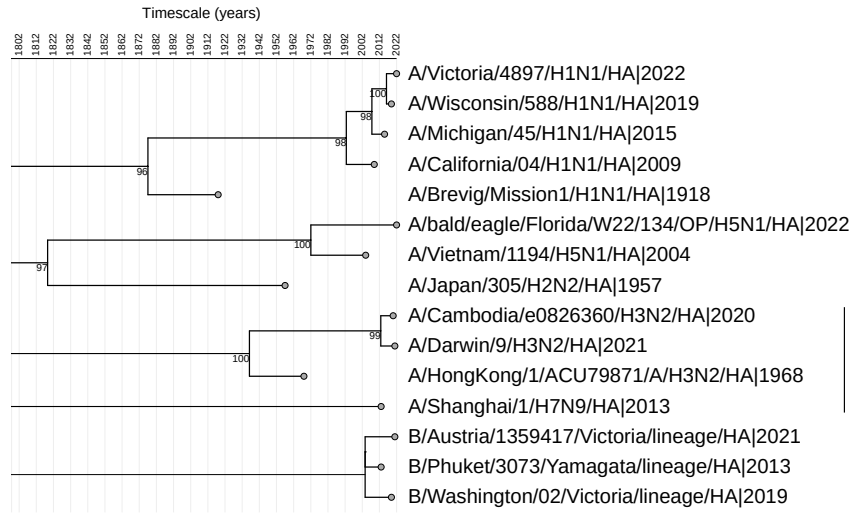


Strain type

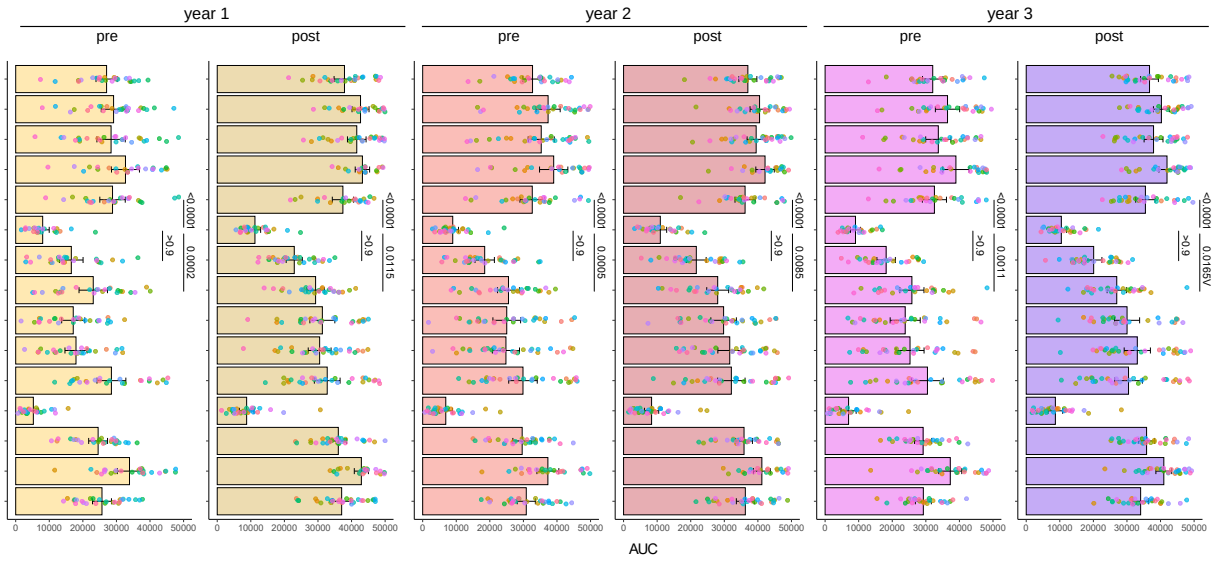
**Figure S13. Comparison of Ig binding responses against Influenza hemagglutinins included vs not included in the seasonal vaccine.**

Multiple Mann-Whitney tests to compare vaccine-induced responses (differences between pre- and post-vaccination) against Influenza hemagglutinins included in the seasonal vaccine of the respective study year (right, vax) vs others that were not included (left, non-vax). Both groups are plotted next to each other in each panel, shown both as violin plots and dot plots, colored by antigen and year. Horizontal black lines indicate the means. Corrections for multiple comparisons were done using the Benjamin-Hochberg method, and adjusted p values are indicated (\*  $p < 0.01$ ), as well as absolute differences (diff) and fold changes of mean dAUCs between vax and non-vax strains. dAUC: difference in area under the curve between pre- and post-vaccination time points.

### A Time tree, all HA antigens



### B binding levels over time



### C vaccine-induced responses

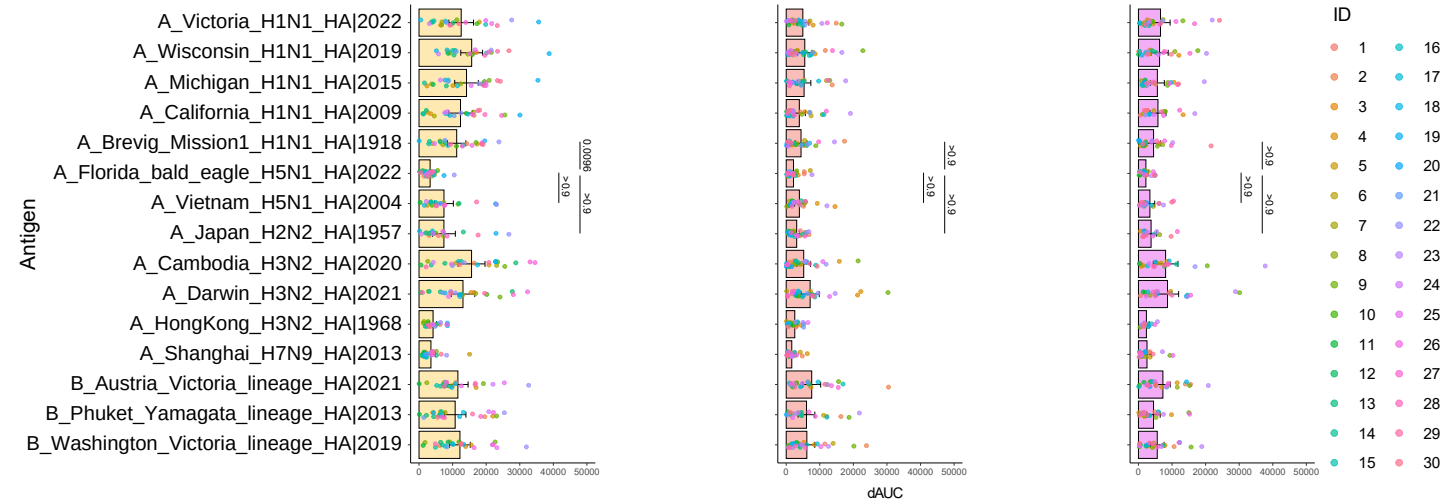
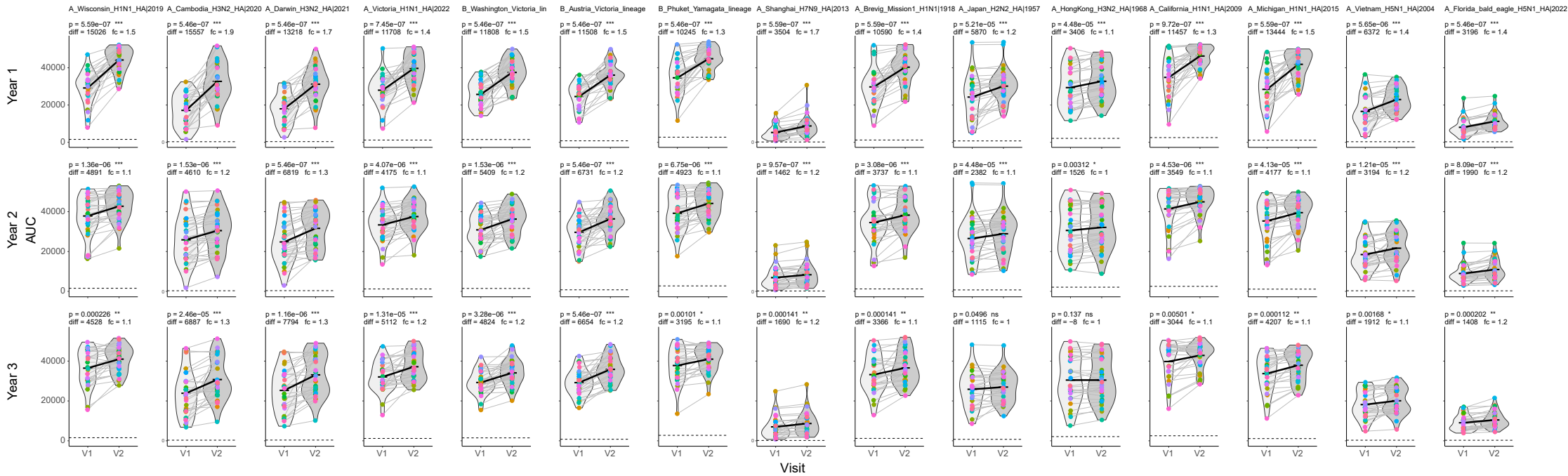


**Figure S14. Anti-hemagglutinin Influenza responses by phylogenetic relatedness.**

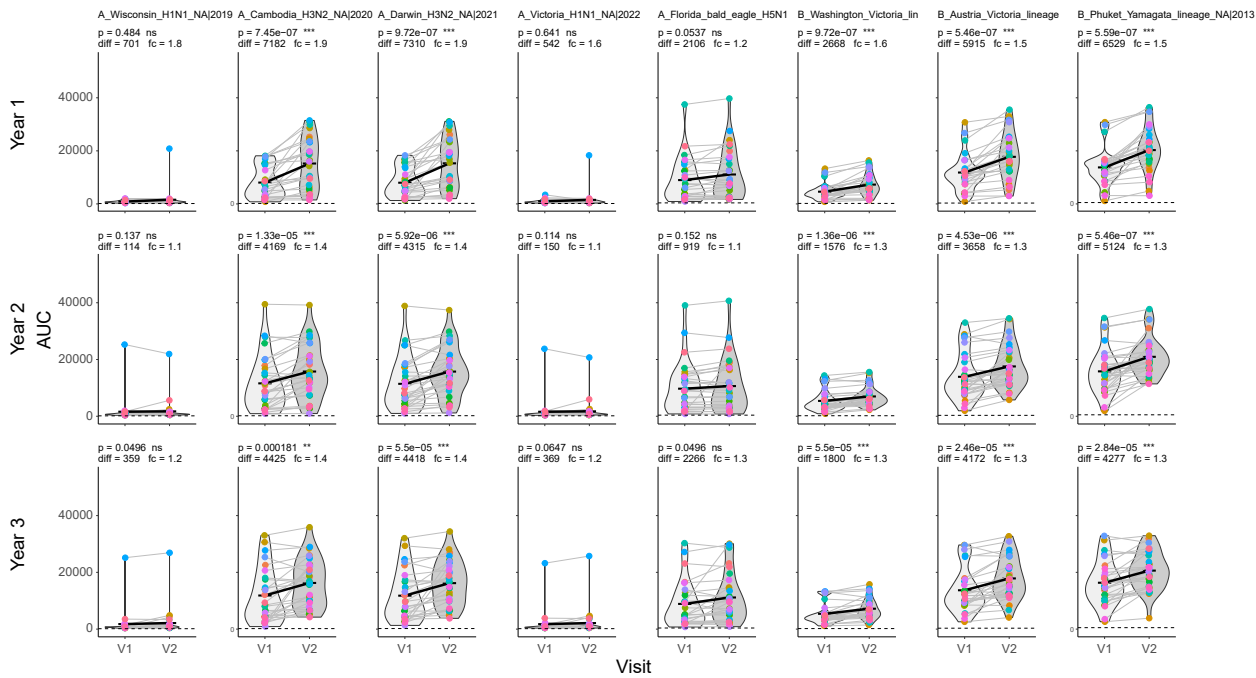
**A.** Time-calibrated maximum-likelihood tree as in **Figure 2B** using sequences of the studied HA antigens across (sub)types and groups. **B.** Ig binding levels shown as horizontal bar graph (means with standard deviation), aligned with the tree sequences in **A**. Graphs are shown for pre- and post-vaccination levels in all three study years. The individual data points are shown as dots colored by participant. **C.** Vaccine-induced responses (differences between pre- and post-vaccination visit) are plotted in the same manner, aligned below each year's visit-specific responses in **B**. Selected non-parametric Kruskal-Wallis tests with Dunn's multiplicity correction are shown, i.e., for A/Florida/H5/2022 (clade 2.3.4.4b) against neighboring H1, H2, and H5 antigens (adjusted p values).

## A Hemagglutinin - recent vaccine strains



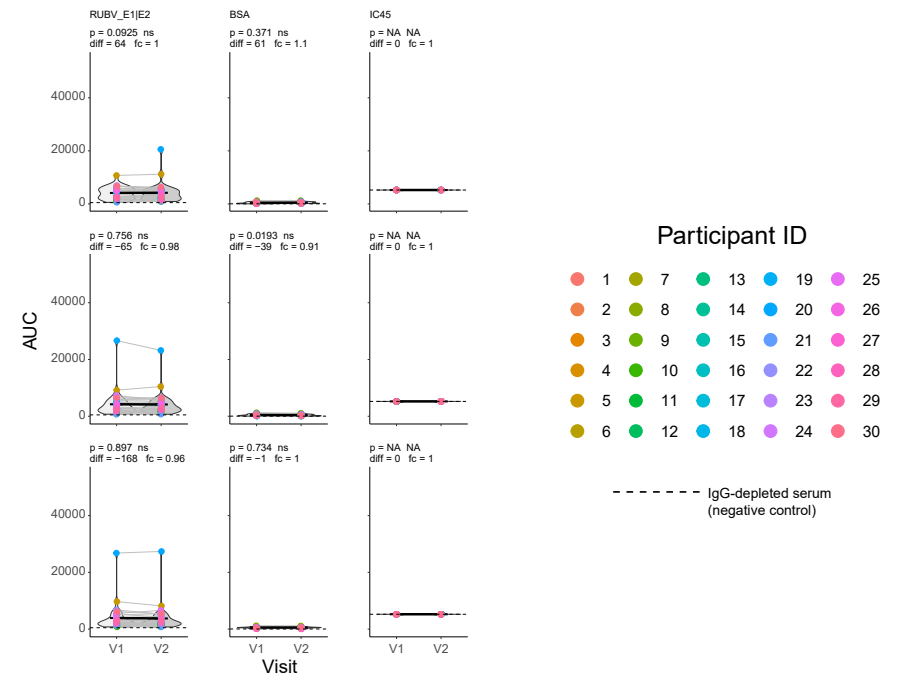
Visit

## C Neuraminidase



Visit

## D Controls



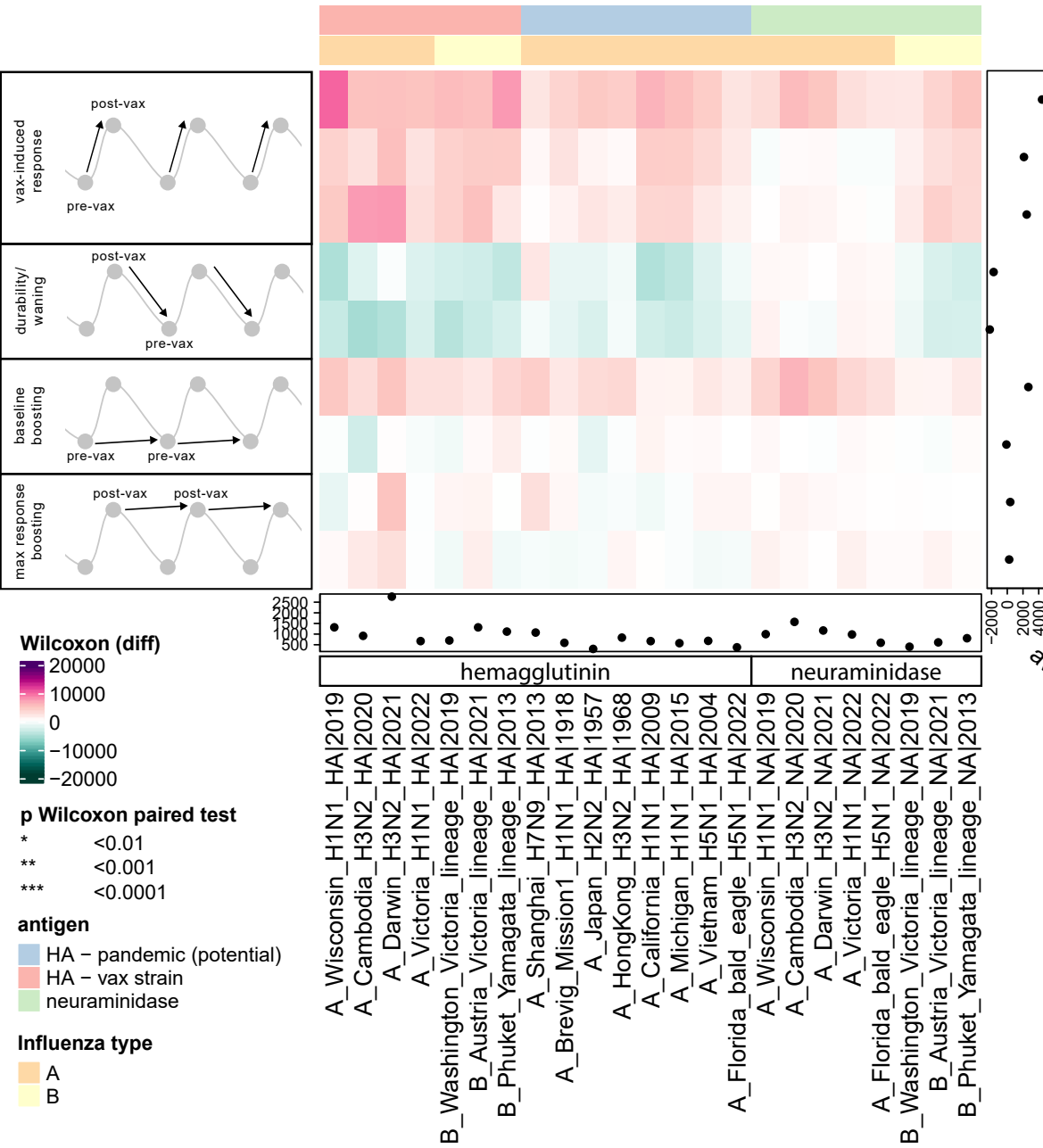
Participant ID



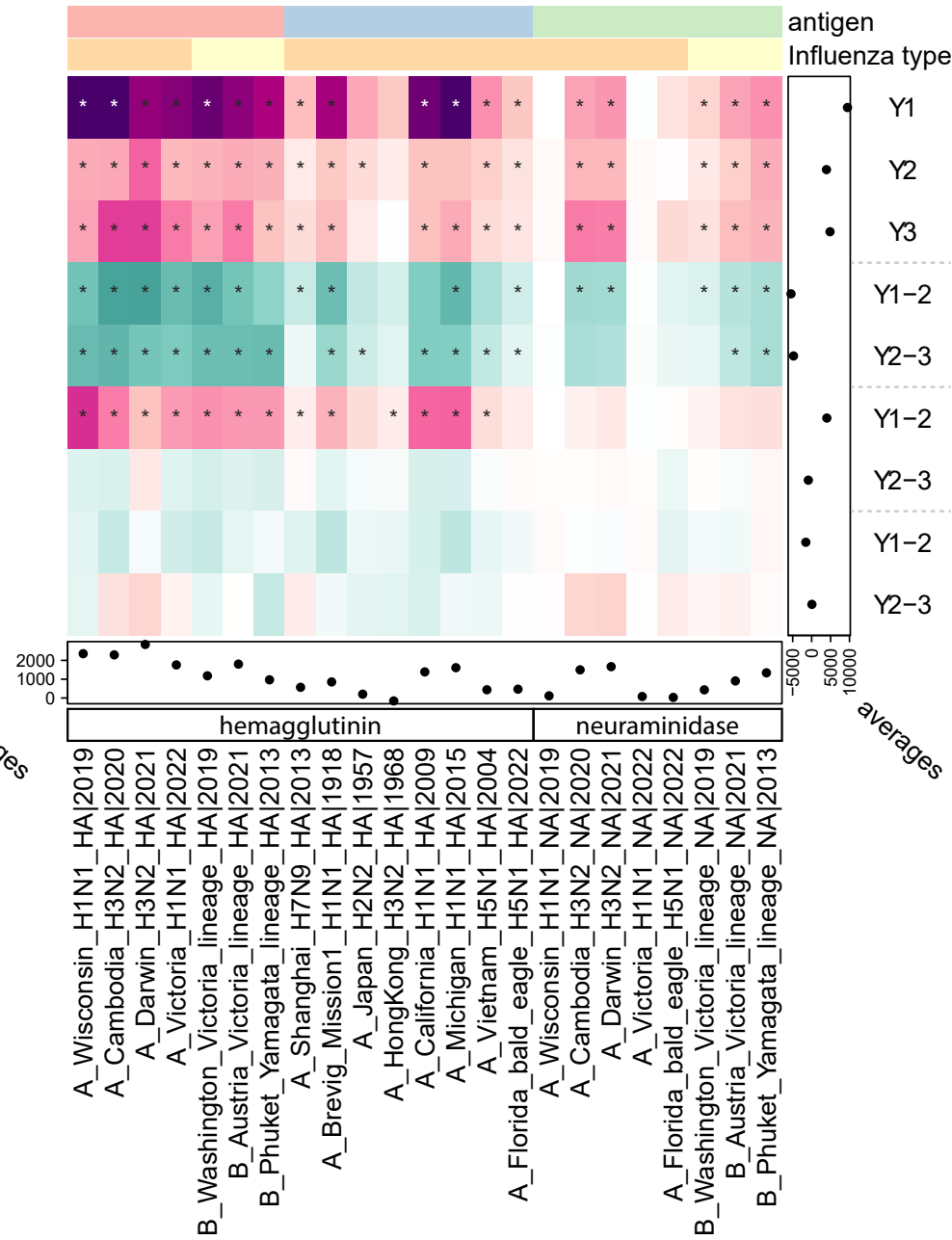
**Figure S15. Vaccine-induced responses by antigen and study year.**

Multiple Wilcoxon paired tests were done to study vaccine-induced responses against each antigen in each year. The pre-vaccination/baseline (V1) and approximately 1-month post-vaccination time points (V2) are plotted next to each other in each panel, shown both as violin plots and dot plots, colored by participant. Linked data points (longitudinal samples of same participant) are connected by gray lines, and the average responses are connected by a bold black line. Corrections for multiple comparisons were done using the Benjamin-Hochberg method, and adjusted p values (\*  $p < 0.01$ , \*\*  $p < 0.001$ , \*\*\*  $p < 0.0001$ ), absolute differences (diff) in AUC ( $\Delta V1V2$ ), and fold changes (fc) are indicated. The dashed line represents the response obtained with IgG-depleted serum as reference. AUC: area under the curve.

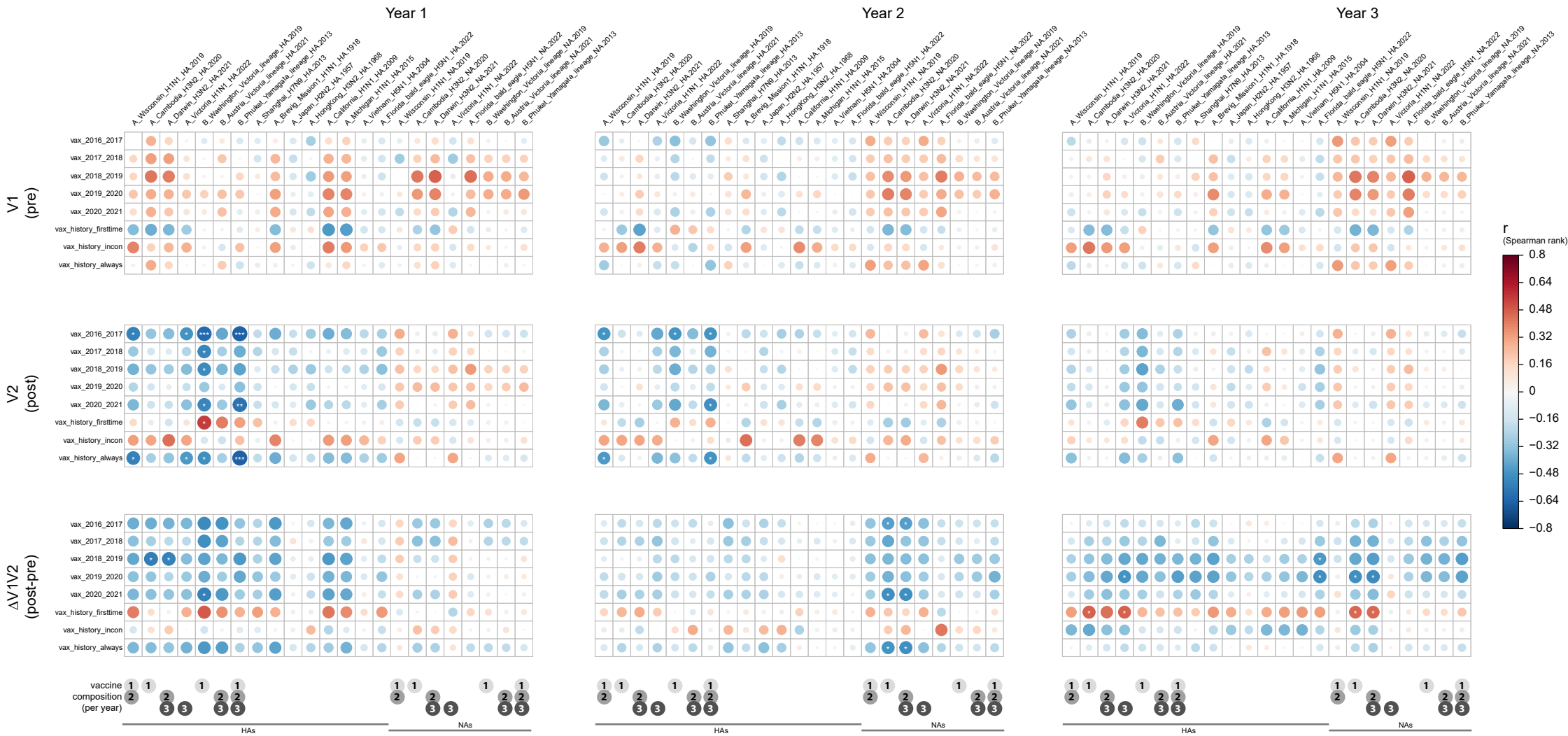
# A always vaccinated (n=7)



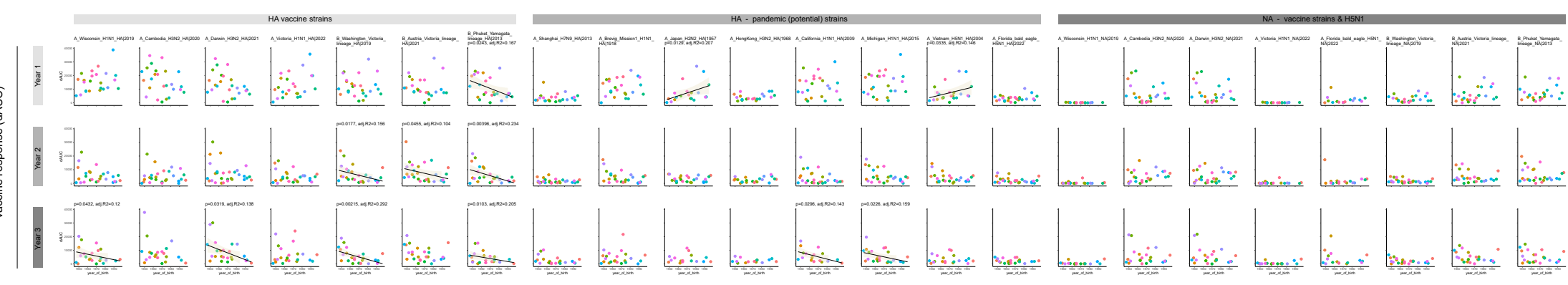
# B first-time vaccinated (n=13)



**Figure S16. Vaccination response dynamics by vaccination history.** Multiple Wilcoxon paired tests as in **Figure 4A** but split according to vaccination history in the five years before study start into participants who were always vaccinated (all five years) (**A**) and first-time vaccinated (**B**). Studied responses from top to bottom are: 1) vaccine-induced responses in each year (top), 2) waning to the following year, 3) boosting of baseline levels to the next year, and 4) changes in maximum (1-month post vax) responses to the next year (bottom). Corrections for multiple comparisons were done separately for 1) – 4) using the Benjamin-Hochberg method. Average responses per heatmap row and column are shown as dot plot to the right and bottom, respectively. The analyses were done by antigen, with Ig responses averaged across participants. Resp: response; vax: vaccination; Y: year.



**Figure S17. Impact of vaccination history on antigen-specific Ig binding responses.** The impact of previous vaccination was analyzed in all study years at time points pre-vaccination (top, V1), 1-month post-vaccination (middle, V2), and for vaccine-induced responses (bottom, dV1V2). Vaccination history referred to the five years before study start (y-axis; individual years or summed up as first-time, inconsistent, or always vaccinated), analyzed across all antigens (x-axis). Spearman rank correlations are summarized in correlograms, where red and blue colors indicate positive and negative correlations, respectively. The color intensity and size of circles indicate correlation strength. White asterisks indicate significance (\*  $p < 0.05$ , \*\*  $p < 0.01$ , \*\*\*  $p < 0.005$ ). The gray spheres at the bottom indicate which antigens were included in the seasonal vaccine for the respective year.

**A****B**

**Figure S18. Serological imprinting by year of birth across multiple antigens and study years, shown as linear regressions.**

Multiple linear regression analysis of Ig binding levels (A) or vaccine-induced responses (differences between pre- and post-vaccination) (B) on the y-axis by year of birth on the x-axis. Individual data points are shown as dots, colored by participants. Corrections for multiple comparisons were done using the Benjamin-Hochberg method, and adjusted p values are indicated. Significant results ( $p < 0.05$ ) are shown with regression line, including 95% confidence interval and goodness-of-fit (R-squared). The dashed line represents the response obtained with IgG-depleted serum as reference. AUC: area under the curve. dAUC: difference in AUC between pre- and post-vaccination time points.

**A**

binding levels (AUC)



**B**

vaccine response (dAUC)

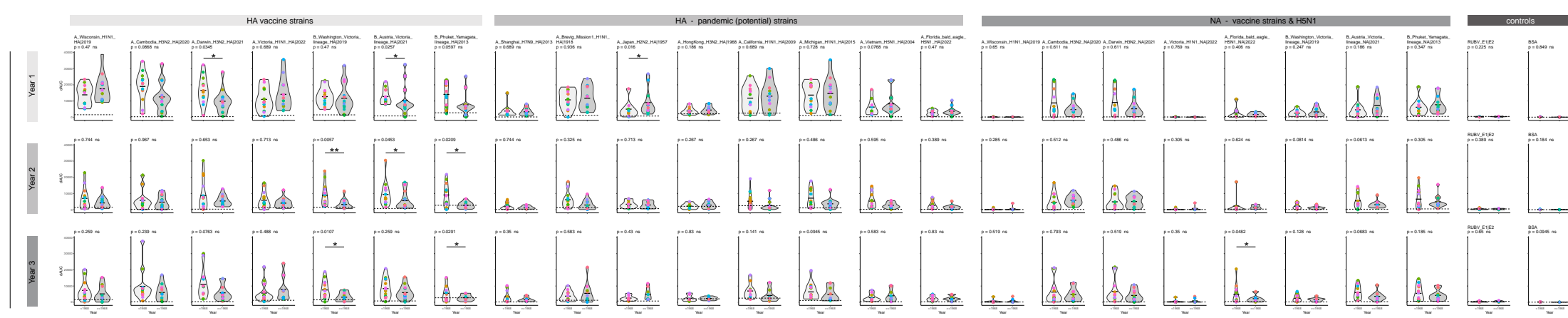


**Figure S19. Serological imprinting by year of birth, shown side-by-side comparing individuals born <1968 and ≥1968.**

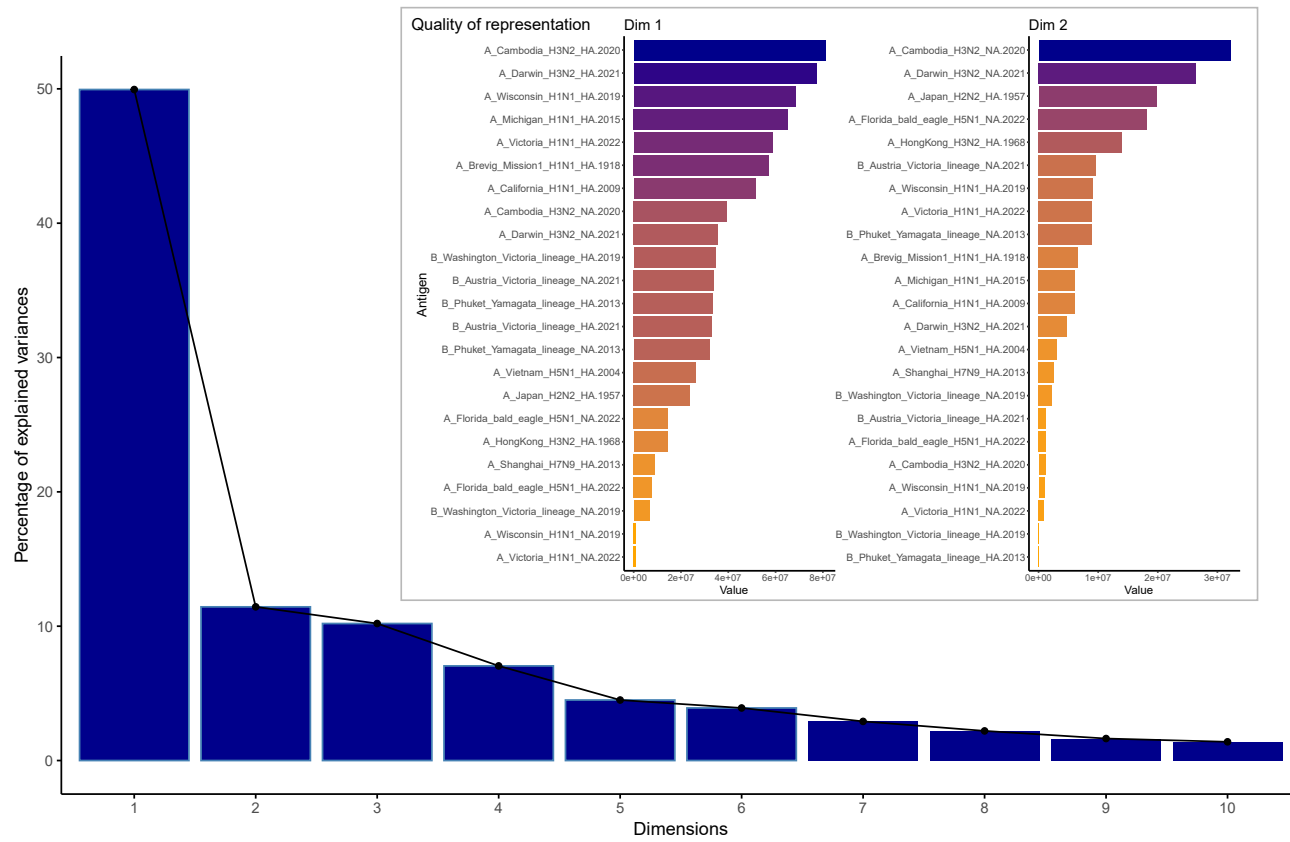
Multiple Mann-Whitney tests to compare binding levels (A) or vaccine-induced responses (differences between pre- and post-vaccination) (B) in participants born <1968 and ≥1968. Both groups are plotted next to each other in each panel, shown both as violin plots and dot plots, colored by participant. Corrections for multiple comparisons were done using the Benjamin-Hochberg method, and adjusted p values are indicated (\* p<0.05). The dashed line represents the response obtained with IgG-depleted serum as reference. AUC: area under the curve. dAUC: difference in AUC between pre- and post-vaccination time points.



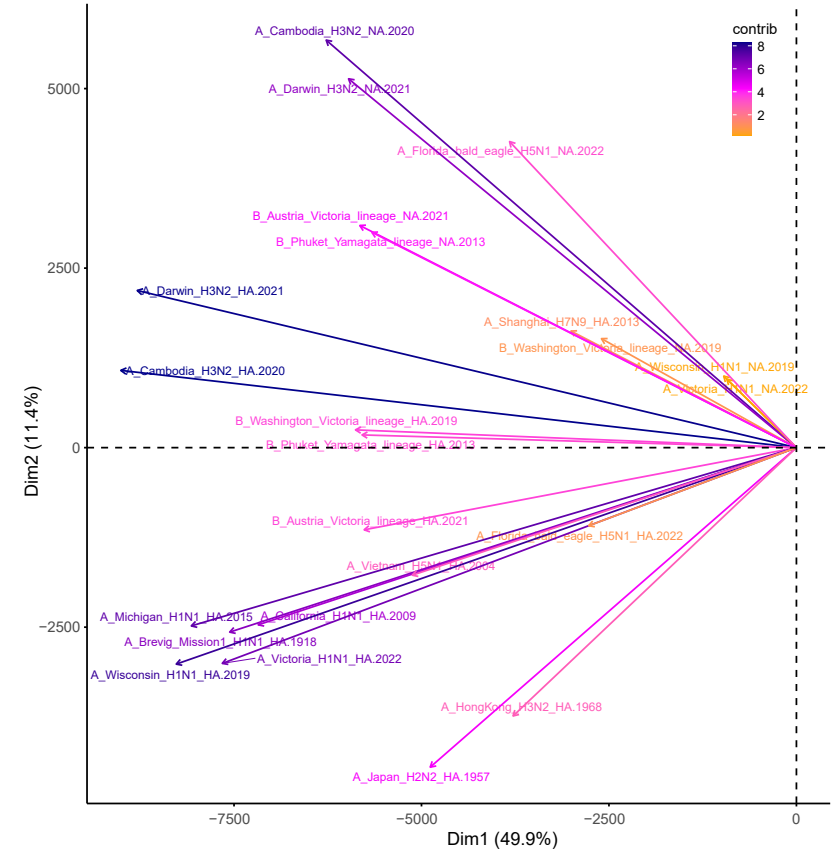
**Figure S20. Correlation analysis of antigen-specific binding responses, clinical, and demographic information.**

Multivariable correlation analyses of anti-Influenza binding responses (x-axis) against selected clinical and demographic variables (y-axis) at baseline/pre-vaccination (top), approximately 1-month post-vaccination (middle), and for vaccine-induced responses (bottom, difference between pre- and post-vaccination levels). Spearman rank correlations are summarized in correlograms, where red and blue colors indicate positive and negative correlations, respectively. The color intensity and size of circles indicate correlation strength. White asterisks indicate adjusted significance after Benjamini-Hochberg multiplicity correction (\*  $p < 0.05$ , \*\*  $p < 0.01$ , \*\*\*  $p < 0.005$ ). The gray spheres at the bottom indicate which antigens were included in the seasonal vaccine for the respective year. Sex: male vs female. Total of  $n=90$  data points from 30 participants over 3 years.

### A PCA - explained variance by dimension



### B Variables - PCA



### C PCA - by year, vax history, and visit

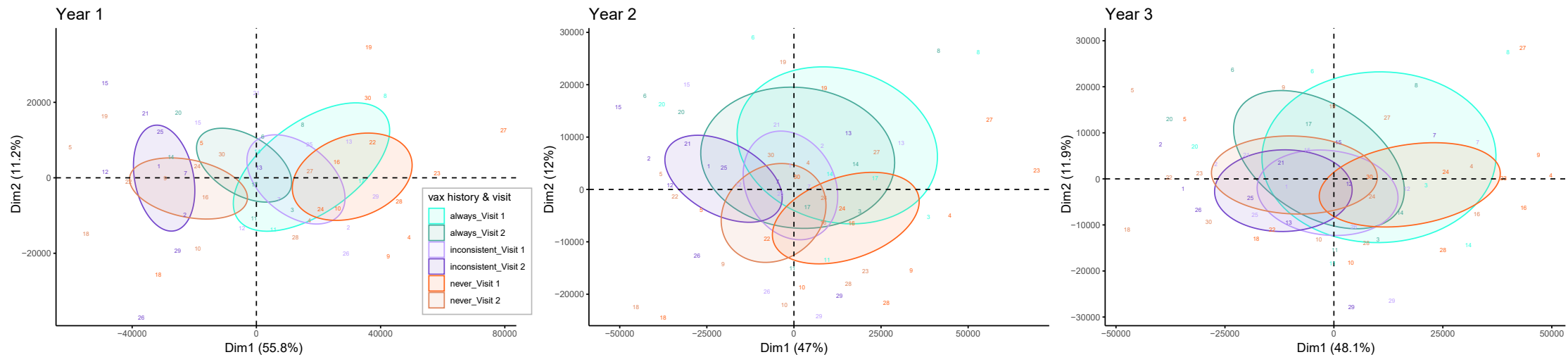
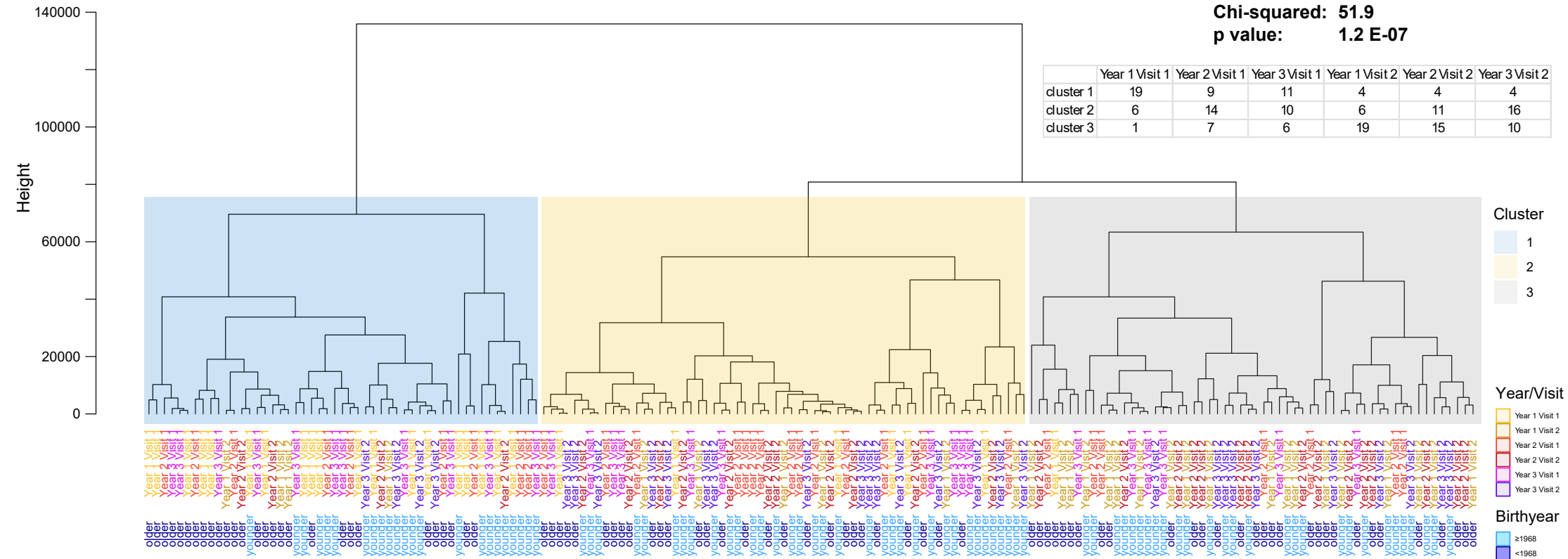


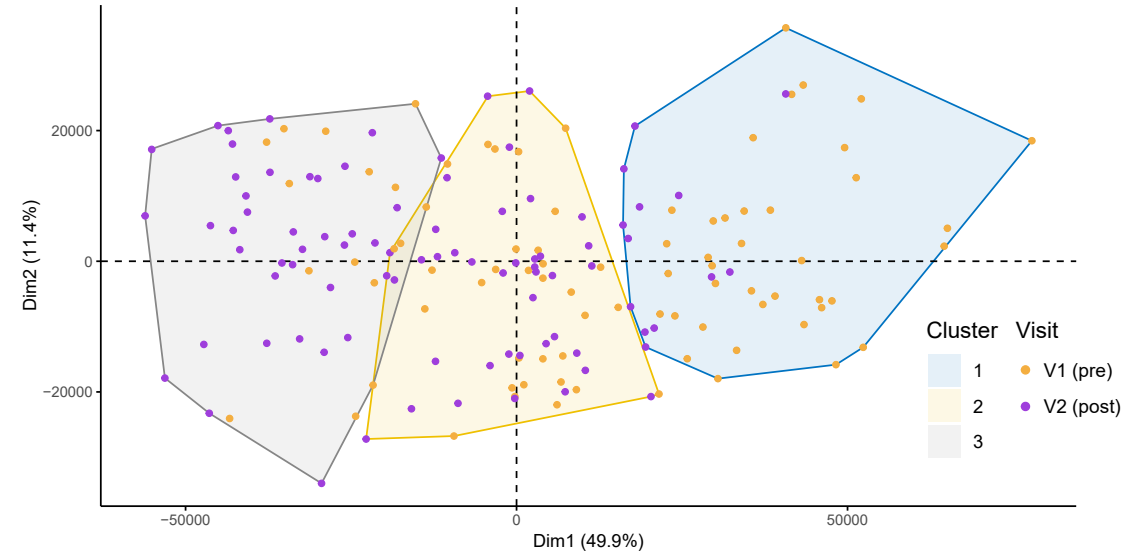
**Figure S21. Principal component analysis (PCA) of multiplex binding responses.**

**A.** PCA of 23 anti-Influenza Ig responses (against 15 HA and 8 NA antigens), with explained variance shown by dimension. Boxed areas indicate the quality of representation for dimensions 1 and 2, which were used in further analysis. The data include 30 participants from the NYU StopFlu vaccination cohort, with 172 total visits collected pre- and post-vaccination over three years. **B.** Variable plot illustrating the contribution strength and direction of the 23 variables in dimensions 1 and 2. **C.** PCA segmented by influenza vaccination history (based on 5 years before study start) and visit (visit 1: pre-vaccination; visit 2: approximately 1 month post-vaccination), displayed for all three study years from left to right. Ellipses depict 95% confidence intervals of the means.

# A PCA-based hierarchical clustering



# B by visit



# C by birth year

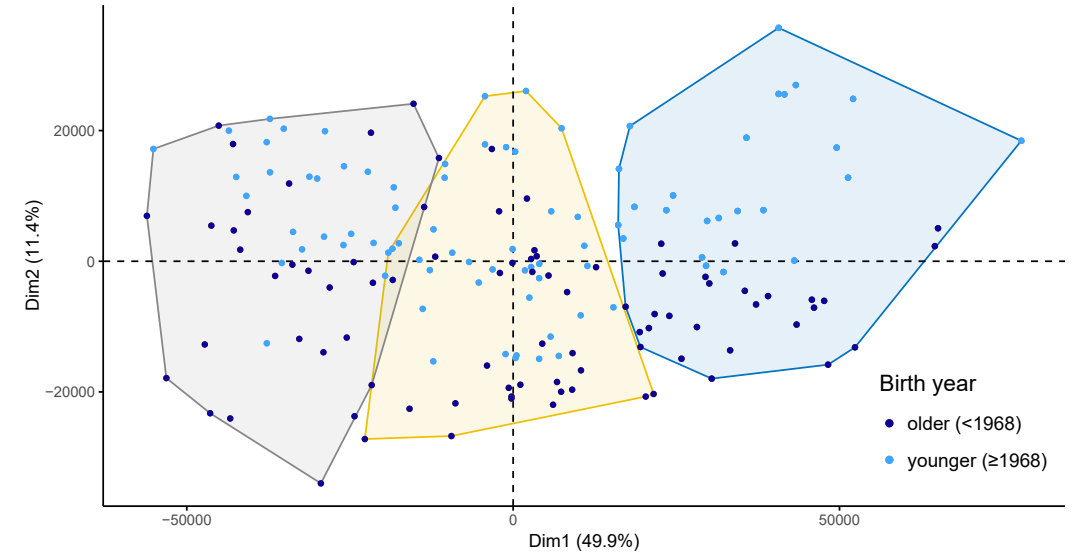
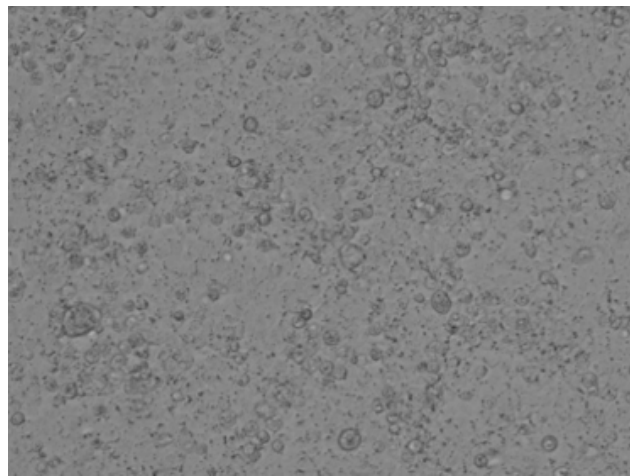
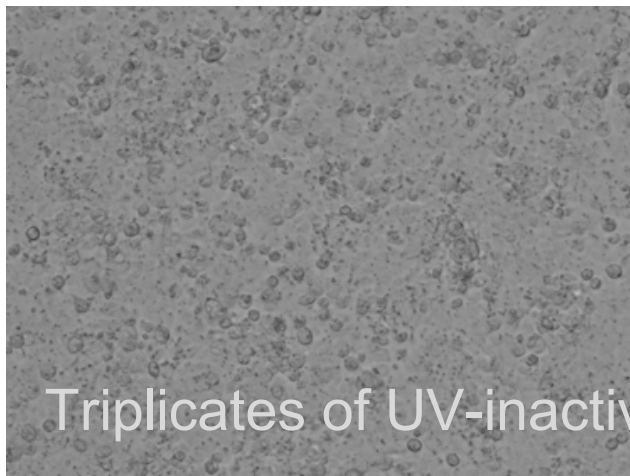
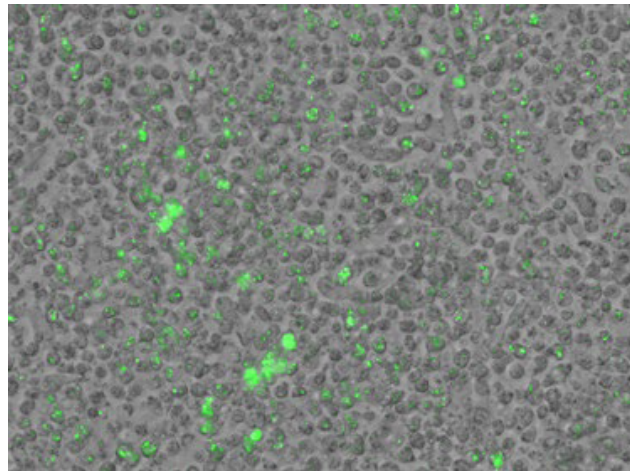
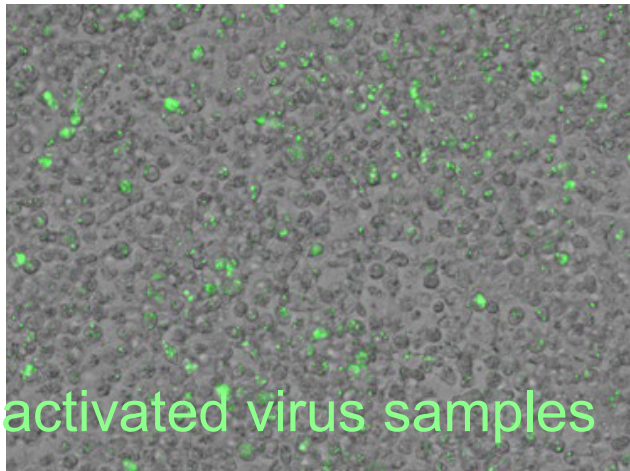
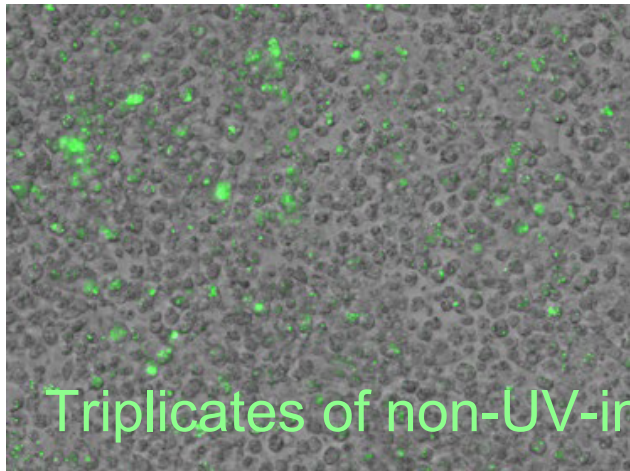


**Figure S22. PCA-based hierarchical clustering.**

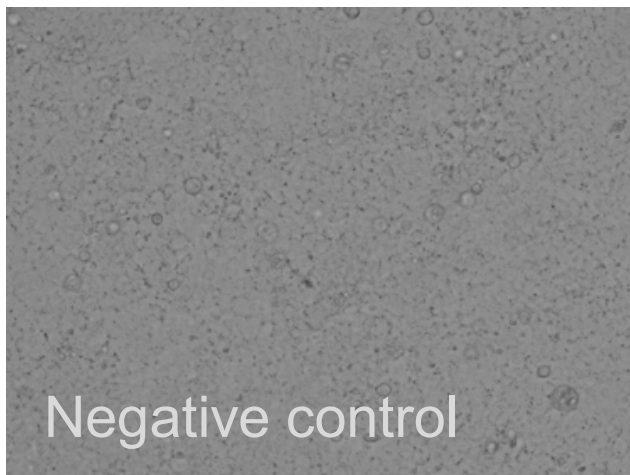
**A.** PCA-based k-means hierarchical clustering of the first two principal components, using the same data set of 23 multiplex anti-Influenza Ig responses (against 15 HA and 8 NA antigens) on 172 data points as in **Fig. 21**. In the dendrogram, the clusters are highlighted with colored boxes; data points are labeled by year/visit (visits 1 and 2 staggered) and birth year, stratified into earlier than 1968 (older) or 1968 and later (younger). **B,C.** The 2-dimensional positioning of data points by visit (**B**) and birth year (**C**) in relation to the clustering.



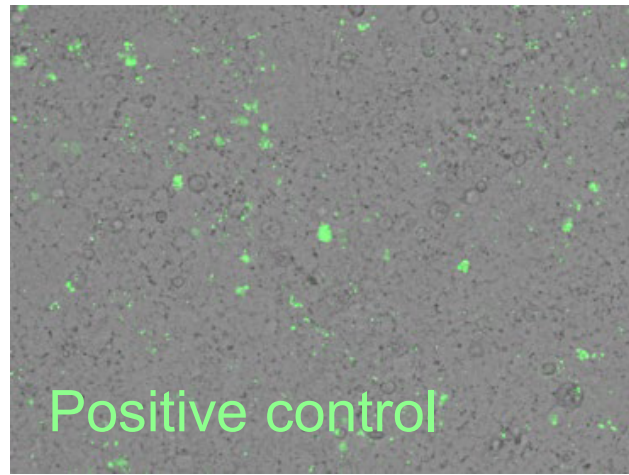
Triplicates of UV-inactivated virus samples



Triplicates of non-UV-inactivated virus samples



Negative control



Positive control

**Figure S23. UV-inactivation of H5N1 mouse immune sera.**

Immune serum obtained from mice challenged and vaccinated with H5N1 virus was UV-inactivated before conducting serological analyses. The inactivation process involved exposing the samples to UV light for 20 minutes (using a UV lamp with a 254 nm wavelength, 6 watts, positioned 3-5 cm above the samples). A positive control, PR8 GFP reporter virus, was included in the inactivation process, while the negative control contained no virus. After UV inactivation, the samples were inoculated onto MDCK cells, and the GFP signal was checked after 24 hours.